

# Gene Networks

## The Influence of Interaction on the Dynamics of Gene Networks

R.W. van Weelden





# Gene Networks

## The Influence of Interaction on the Dynamics of Gene Networks

by

Rick van Weelden

to obtain the degree of Bachelor of Science  
at the Delft University of Technology,  
to be defended publicly on Wednesday July 28, 2021 at 13:00.

Student number: 4875966  
Project duration: March 21, 2021 – July 28, 2021  
Thesis committee: dr. J.L.A. Dubbeldam, TU Delft, supervisor  
dr. B. van der Dries, TU delft, assessor

An electronic version of this thesis is available at <http://repository.tudelft.nl/>.



# Preface

This thesis has been written as the final requirement to obtain the degree of Bachelor of Science in Applied Mathematics at Delft University of Technology. As a third year applied mathematics student, I have worked on this project for several months in Q4.

While writing this report I assumed the reader to have the knowledge of a third year mathematics student, in particular some basic knowledge of Linear Algebra, Probability Theory, Differential Equations and Numerical Methods.

As you might have seen the title contains the word 'network'. Network theory does have a huge role in this thesis. However, readers need not be familiar with network theory, as the basics will be discussed in Chapter 2.

I would like to thank my supervisor Johan for his support and guidance during this project and for the long weekly meetings, where we shared our thoughts. I would also like to thank Bart for taking a seat in my thesis committee.

*Rick van Weelden  
Reeuwijk, July 2021*



# Layman Summary

Species evolve. Once a Neanderthals, now a Homo sapiens. We are the human race. You might not notice it, but a lot of things evolve around you, even if its small. Evolution is the gradual development of something. Animals, insects, people; they all evolve by interacting with each other and with the environment.

Now these organisms are quite big and visible by the eye, but there are many more organisms. Think of the gut bacteria E.coli or Baker's yeast that is used in baking bread. These organisms are not visible by the eye, but they do exist, they do evolve and they do interact with each other.

For a microbiologist it is interesting how these minuscule organisms interact. As a mathematician we can help the microbiologist in the study of these interactions. We can translate and simplify the reality into an abstract mathematical model by using mathematical language and tools. This mathematical model can then be studied by us, to hopefully find some interesting properties to assist the microbiologist in his study in the interactions of organisms. Which is done in this report.



# Summary

It might surprise you that networks play a role in biology, but networks are ubiquitous. All living things have DNA within their cells. This DNA contains the building blocks of an organism. The process of creating such a building block requires mRNA and proteins. The concentration of a certain mRNA molecule plays a part in the making of these proteins. In biology these processes are called transcription and translation. These interacting processes can be transformed into a mathematical model, a network. This network is a collection of nodes and edges, which represent the interactions between different mRNA concentrations. Since these interactions are unknown, random matrix theory is used to model these interactions. It is interesting how the concentrations of mRNA molecules evolve over time. A system of differential equations can be used to model these changes of concentrations over time.

This report aims to discover the properties of the model of interacting organisms. For this a linear model is found, which is a system of differential equations linearised around a given equilibrium. A system can be written as a matrix, to model multiple organisms this results in a block matrix. Each block can then be envisioned to model a certain gene pool that corresponds to an organism. Interactions between these gene pools can be modelled by adding an interaction block to the off diagonal blocks of the block matrix. Later on this linear model is improved with a non-negative constraint, concentrations are after all non-negative, which results in a new nonlinear model.

Properties of both models are found by studying the distribution of the eigenvalues. Girko's law and Wigner's law are two important laws from random matrix theory, that help with the determination of the eigenvalues of a random interaction matrix. For the linear model it was found that the distribution of the eigenvalues is influenced by the entries of the block matrix and by the strength of the connection between the block matrices. Once the eigenvalues and the corresponding eigenvectors are found, the solution is deterministic. For the nonlinear model it was found that the distribution of the eigenvalues are influenced in a similar way as the linear model. But due the non-negative constraint, the stability of the system is not deterministic. The system can be partly asymptotically stable, partly stable and partly unstable for different time windows. It is living on the 'edge of chaos'.



# Contents

|          |  |           |
|----------|--|-----------|
| <b>1</b> | <b>Introduction</b>                                      | <b>1</b>  |
| <b>2</b> | <b>Gene Network</b>                                      | <b>3</b>  |
| 2.1      | Network Theory . . . . .                                 | 3         |
| 2.1.1    | Graph . . . . .  | 3         |
| 2.1.2    | Adjacency Matrix and Connectivity . . . . .              | 4         |
| 2.2      | Biological Model for Gene Networks. . . . .              | 4         |
| 2.2.1    | Derivation of the Linear Differential Equation . . . . . | 5         |
| 2.2.2    | Erdős–Rényi Model . . . . .                              | 6         |
| <b>3</b> | <b>Distribution of Eigenvalues: Random Matrix Theory</b> | <b>9</b>  |
| 3.1      | Wigner’s Semicircle Law . . . . .                        | 9         |
| 3.2      | Girko’s Law . . . . .                                    | 13        |
| 3.2.1    | Center. . . . .  | 14        |
| 3.2.2    | Radius. . . . .  | 15        |
| <b>4</b> | <b>Linear Model for Gene Networks</b>                    | <b>17</b> |
| 4.1      | Stability of Solutions . . . . .                         | 19        |
| 4.2      | Independent Networks . . . . .                           | 19        |
| 4.2.1    | Note on the Numerical Solution . . . . .                 | 21        |
| 4.3      | Interacting Networks: The Interconnection . . . . .      | 21        |
| 4.3.1    | Interconnection of Weight One. . . . .                   | 21        |
| 4.3.2    | Small Interconnection . . . . .                          | 24        |
| 4.3.3    | Large Interconnection . . . . .                          | 25        |
| 4.3.4    | Directed Interconnection . . . . .                       | 26        |
| 4.3.5    | The Number and Placement of Interconnections . . . . .   | 28        |
| 4.4      | Strictly Positive Interaction Matrix . . . . .           | 31        |
| 4.5      | Strictly Negative Interaction Matrix . . . . .           | 33        |
| <b>5</b> | <b>Nonlinear Model for Gene Networks</b>                 | <b>35</b> |
| 5.1      | Numerical Solutions of the Nonlinear Model . . . . .     | 35        |
| 5.1.1    | Interconnection of Weight One. . . . .                   | 36        |
| 5.1.2    | Large Interconnection . . . . .                          | 36        |
| 5.1.3    | Strictly Positive Interaction Matrix . . . . .           | 37        |
| 5.1.4    | Strictly Negative Interaction Matrix . . . . .           | 38        |
| 5.2      | On and Off Distribution of Nodes . . . . .               | 39        |
| 5.3      | Maximal Lyapunov Exponent . . . . .                      | 41        |
| 5.3.1    | Edge of Chaos . . . . .                                  | 41        |
| 5.3.2    | Size of Network. . . . .                                 | 42        |
| 5.3.3    | Weight and Amount of Interconnections. . . . .           | 43        |
| 5.4      | Initial Condition . . . . .                              | 45        |
| <b>6</b> | <b>Discussion</b>  | <b>47</b> |
| <b>7</b> | <b>Conclusion</b>  | <b>49</b> |
| 7.1      | Linear Model . . . . .                                   | 49        |
| 7.2      | Nonlinear Model . . . . .                                | 49        |
| 7.3      | Recommendations . . . . .                                | 50        |
| <b>A</b> | <b>Notes on the Proof of Wigner’s Semicircle</b>         | <b>51</b> |



# List of Figures

|      |   |    |
|------|---|----|
| 2.1  | Directed weighted graph with loops . . . . .  | 4  |
| 2.2  | Scheme of biological reactions on molecular scale . . . . .   | 5  |
| 2.3  | Graph to construct the adjacency matrix . . . . .   | 7  |
| 2.4  | Weighted graph to construct the interaction matrix . . . . .  | 7  |
| 3.1  | Simulation of Wigner's semicircle . . . . .   | 10 |
| 3.2  | Girko's and Wigner's law . . . . .  | 14 |
| 3.3  | Shifted Girko's circle . . . . .  | 15 |
| 3.4  | Radius of Girko's circle depending on $\sigma$ . . . . .  | 16 |
| 3.5  | Radius of Girko's circle depending on $\langle k \rangle$ . . . . .   | 16 |
| 4.1  | Graphical representation of the Gene network of Yeast . . . . .   | 18 |
| 4.2  | Stability of solutions: Divergent, oscillatory and convergent . . . . .   | 19 |
| 4.3  | Eigenvalue distribution of two independent networks consisting of 4 nodes each . . . . .                        | 20 |
| 4.4  | Linear numerical solution for two independent networks . . . . .  | 21 |
| 4.5  | Graphical representation of an interacting network of weight $\epsilon$ . . . . .                               | 22 |
| 4.6  | Eigenvalue distribution of two interconnected networks with interconnection weight $\epsilon = 1$ . . . . .     | 22 |
| 4.7  | Linear numerical solution of two interconnected networks with interconnection weight $\epsilon = 1$ . . . . .   | 23 |
| 4.8  | Eigenvalue distribution of two interconnected networks with interconnection weight $\epsilon = 0.1$ . . . . .   | 24 |
| 4.9  | Linear numerical solution of two interconnected networks with interconnection weight $\epsilon = 0.1$ . . . . . | 24 |
| 4.10 | Eigenvalue distribution of two interconnected networks with interconnection weight $\epsilon = 3$ . . . . .     | 25 |
| 4.11 | Linear numerical solution of two interconnected networks with interconnection weight $\epsilon = 3$ . . . . .   | 26 |
| 4.12 | Numerical Solution Directed interconnection to network 1 . . . . .  | 27 |
| 4.13 | Numerical Solution Directed interconnection to network 2 . . . . .  | 27 |
| 4.14 | Histogram of eigenvalue distribution of real parts for randomly interconnected networks . . . . .               | 28 |
| 4.15 | Histogram of eigenvalue distribution of real parts for 4 interconnections placed randomly . . . . .             | 29 |
| 4.16 | Eigenvalue distribution of a network with 4 interconnections in 4 distinct rows and columns . . . . .           | 30 |
| 4.17 | Eigenvalue distribution of a network with 4 interconnections in 3 distinct rows and columns . . . . .           | 30 |
| 4.18 | Eigenvalue distribution of a network with 16 interconnections . . . . .   | 31 |
| 4.19 | Linear numerical solution for a strictly positive interaction matrix . . . . .                                  | 32 |
| 4.20 | Linear numerical solution for a strictly positive interaction matrix with $\mathbf{x}_0 = 999$ . . . . .        | 32 |
| 4.21 | Linear numerical solution for a strictly negative interaction matrix . . . . .                                  | 33 |
| 5.1  | Linear vs nonlinear numerical solution with interconnection weight $\epsilon = 1$ . . . . .                     | 36 |
| 5.2  | Linear vs nonlinear numerical solution with interconnection weight $\epsilon = 3$ . . . . .                     | 37 |
| 5.3  | Linear vs nonlinear numerical solution for a strictly positive interaction matrix . . . . .                     | 38 |
| 5.4  | Linear vs nonlinear numerical solution for a strictly negative interaction matrix . . . . .                     | 38 |
| 5.5  | (Average) On and off distribution of nodes . . . . .  | 39 |
| 5.6  | On and off node distribution for $N=200$ and $D=0.6$ . . . . .  | 41 |
| 5.7  | Edge of chaos for different values of $D$ . . . . .   | 42 |
| 5.8  | Lyapunov for different network sizes $N$ up to 500 . . . . .  | 43 |
| 5.9  | Lyapunov for different network sizes $N$ up to 800 . . . . .  | 43 |
| 5.10 | Lyapunov for one interconnection of different weight $\epsilon$ up to $\epsilon = 0.5$ . . . . .                | 44 |
| 5.11 | Lyapunov for one interconnection of different weight $\epsilon$ up to $\epsilon = 1$ . . . . .                  | 44 |
| 5.12 | Lyapunov for ten interconnections of different weight $\epsilon$ up to $\epsilon = 0.5$ . . . . .               | 45 |
| 5.13 | Lyapunov for different initial conditions $\mathbf{x}_0$ . . . . .  | 45 |
| 5.14 | (Average) On and off distribution of nodes for $\mathbf{x}_0 = 999$ . . . . .                                   | 46 |



# 1

## Introduction

Fully understanding organisms on molecular scale is the dream of any microbiologist. Humans, animals and bacteria, each of them have DNA, a gene pool. This DNA codes via mRNA for several proteins. The proteins are the building blocks of an organism, they are involved in chemical reactions, in the transport of other molecules and in the looks of an organism. On molecular level the mRNA molecules and proteins interact with each other. All these interactions can be translated to a network, a collection of nodes and edges.

In theory, if you would exactly know how these interactions work, then you could predict the characteristics of an organism or you could modify it in such a way to get a desired trait of the organism. For us these ideas are too ambitious. We simply do not know how the interactions work on molecular scale or how different organisms, like bacteria, interact with each other. We should get a grasp of it. This is where a mathematical model comes into play. Such a model is a simplification of the reality, but it could simulate the interactions on molecular level, this results in a so called interaction matrix. This model can then be studied to get an understanding of the interactions within and between organisms.

The aim of this report is to study the stability of the model for the gene pools of interacting organisms. This is done by studying the eigenvalue distribution of the interaction matrix. Since these interactions are often unknown, we resort to random matrix theory (RMT). In RMT there are several laws, that tells us how the eigenvalues of a random interaction matrix are distributed.

In the use of RMT two problems arise. Firstly, the laws in RMT are given for large matrices of infinite size. For computational reasons, we have to use finite and rather 'small' matrices; at largest a matrix of size 800. Secondly, to model the interaction between organisms, we add a deterministic value to the interaction matrix, which can have a huge influence on the eigenvalue distribution and therefore on the stability of the system, this is not predicted by the RMT laws.

Another problem that arises is the use of a nonlinear model. Since concentrations of molecules are non-negative, this adds the 'concentrations are non-negative'-constraint to the model, which turns a linear model into a nonlinear model. In this case the eigenvalue distribution of the interaction matrix can not be used to determine the stability of the nonlinear model.

The report will have the following structure. Chapter 2 will provide the required theoretical background of biology and network theory to understand the model. Random matrix theory and its important laws for the distribution of eigenvalues is treated in chapter 3. The stability of the linear model for different types of interaction matrices is discussed in chapter 4. In chapter 5 the stability of different types of interaction matrices in the case of the nonlinear model is examined.



# 2

## Gene Network

This chapter aims to introduce the biological model used to simulate a network of genes. In section 2.1 a quick recap is given of some basic definitions in graph theory. In the following section (2.2) the biological model for gene networks is introduced.

### 2.1. Network Theory

In this section a graph, its corresponding adjacency matrix and connectivity are defined. This section can be omitted if the reader is familiar with this basic terminology used in graph theory.

#### 2.1.1. Graph

In mathematics network theory is the study of graphs, where the graph represents some relation between objects. The relation between objects can be symmetric or asymmetric. This depends on the fact whether the relation is mutual or one-sided. A mutual relationship results in a undirected graph, while a one-sided relationship is considered a directed graph. Network theory is a sub-area of graph theory. A graph is an ordered pair of finite sets  $(V, E)$ . The elements of  $V$  are the vertices, also called nodes. The elements of  $E$  are the edges, these are also called links. The edges connect the vertices with each other.

There are many different types of graphs. The most important for this report is the directed weighted graph with loops. In Figure 2.1 an example of such graph is shown.

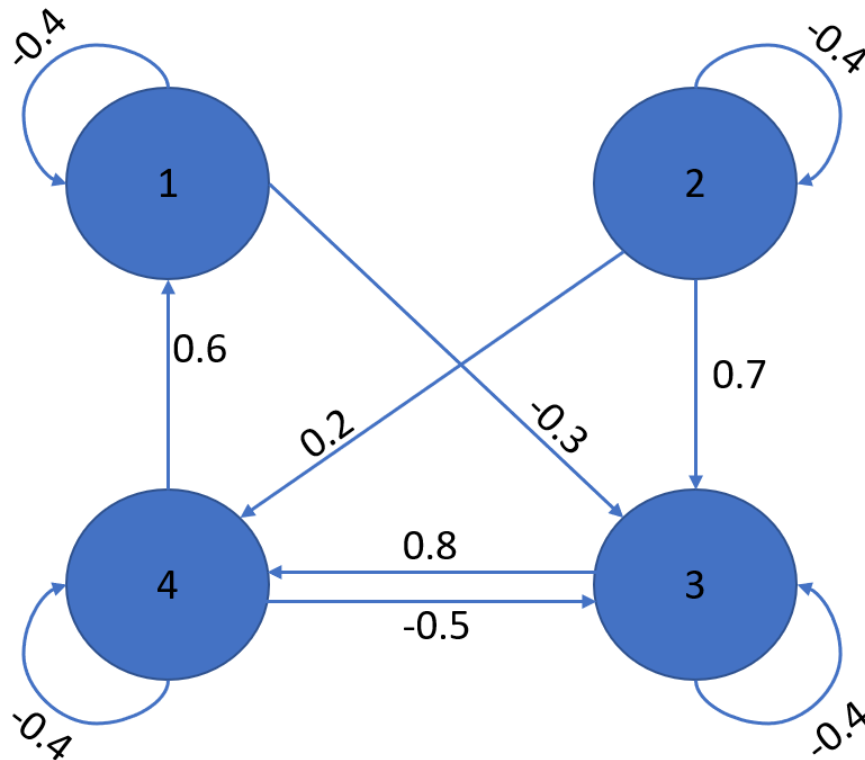


Figure 2.1: An example of a directed weighted graph with loops. The graph consists of the nodes  $\{1,2,3,4\}$  and has directed edges with their corresponding weight next to it.

### 2.1.2. Adjacency Matrix and Connectivity

The directed graph has edges  $(u, v)$  leaving the vertex  $u$  and entering the vertex  $v$ . In above figure (2.1) there is for example an edge leaving vertex 2 and entering vertex 3 with weight 0.8, the edge can then be written as  $(2, 3)$ .

This kind of notation might be useful for mathematical proofs or graphical reasons. However, we wish to do a lot of calculations with these graphs. To do these calculations the matrix of a graph is a useful tool. This matrix is also called the adjacency matrix. In the adjacency matrix all the vertices and their corresponding weights are neatly organised. Writing down the edge  $(3, 4)$  with weight 0.8 in the adjacency matrix gives an entry with value 0.8 in the third row and fourth column. In general the entries  $A_{ij}$  denote the weight of an edge directed from node  $i$  to node  $j$ . Eventually, we obtain the following (weighted) adjacency matrix of Figure 2.1:

$$A = \begin{bmatrix} -0.4 & 0 & -0.3 & 0 \\ 0 & -0.4 & 0.7 & 0.2 \\ 0 & 0 & -0.4 & 0.8 \\ 0.6 & 0 & -0.5 & -0.4 \end{bmatrix}$$

If the number of nonzero entries in  $A$  is denoted by the connectivity  $L$ , then the average connectivity  $\langle k \rangle = \frac{L}{n}$ . Where  $n$  is the amount of nodes. So, here the connectivity is simply the amount of edges in a graph and the average connectivity defines the average amount of edges per node.

## 2.2. Biological Model for Gene Networks

You might ponder: what does network theory have to do with gene networks? To understand this some biological background is required. A gene network is a representation of genes, or in our case one step further the gene products: mRNA transcripts and proteins. In Figure 2.2 this scheme is visualised.

A gene is a piece of DNA that contains information about specific proteins. The created proteins are the building blocks of the organism and fulfil a lot of functions within organisms. For humans you

might think of your ears, your eyes and your hair. Besides your look, proteins also do a lot inside your body. For example; they provide structure to your cells, they transport molecules or they play a part in chemical reactions.

Mathematically we wish to model such a network of genes. Assuming that you know the genome of an organism, the function of each protein and their interaction rates, you could model the concentration of proteins over time. However, in reality most of these properties are unknown. Making the mathematical model will therefore require several assumptions and simplifications.

First of all we assume that gene-to-gene interactions can actually be modelled as chemical reactions between proteins, mRNA and other nucleic material (DNA, RNA). We will denote the concentration of mRNA molecule  $i$  at time  $t$  by  $x_i(t)$  and the concentration of protein  $\alpha$  by  $p_\alpha(t)$ . These concentrations can be combined into one vector, lets say,  $\mathbf{y} = (\mathbf{p}, \mathbf{x})$ . Naturally, concentrations are non-negative, which brings a restriction to our model namely:  $\mathbf{y} \geq 0$ . This will make our model slightly non-linear.

Above that, we assume that there exists at least one fixed point  $\mathbf{y}^0$  and that the gene-network is sufficiently smooth. It is known that every smooth system, no matter how non-linear, is approximately linear near its steady state solutions, also known as fixed points. Usually, mRNA directly codes for their proteins, therefore only the vector  $\mathbf{x}$  is taken into account and the gene-to-gene interactions (Figure 2.2) are captured into an interaction matrix, which include the proteins. In subsection 2.2.1 this will be explained more thoroughly.

Now network theory comes into play to translate the model into a graph and its corresponding adjacency matrix. A node represents the concentration of the  $i$ 'th mRNA molecule, while the edges represent the reactions between the mRNA molecules, these reactions are caused by the proteins. After linearisation around the fixed point, we eventually obtain a linear differential equation. Together with the non-negative restriction, this results in the following non-linear model:

$$\begin{aligned} \frac{d}{dt}x_i &= \sum_j A_{ij}(x_j - x_j^0) && \text{[Entrywise]} \\ \frac{d}{dt}\mathbf{x} &= A(\mathbf{x} - \mathbf{x}^0) && \text{[In Matrix form]} \\ x_i &\geq 0 && \text{[Non-negative restriction]} \end{aligned} \tag{2.1}$$

The change in concentration of a certain mRNA molecule depends on the weights of the interaction matrix and the deviation of the mRNA molecules with respect to their equilibrium value. The effect of a certain weight depends on its sign and its magnitude. A negative weight has an inhibitory effect, while a positive weight has an excitatory effect. The magnitude of the weight determines the effect in size. An example of such an interaction matrix is given in subsection 2.2.2. Another assumption is that a mRNA molecule always has an inhibitory effect on itself. Otherwise it is possible that the mRNA molecule keeps increasing its own concentration, which is most of the time due to a defect in the system.

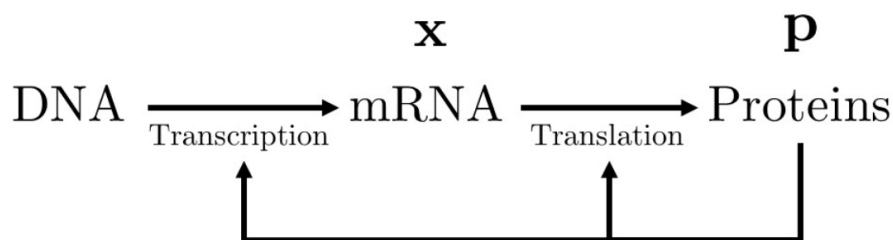


Figure 2.2: "The central dogma of molecular biology. Usually the arrows from the proteins to transcription and translation are not included. Here this interaction is relevant. There are proteins needed to execute transcription and translation."(Sanders, 2020)

### 2.2.1. Derivation of the Linear Differential Equation

In this part a more detailed derivation of the linear differential equation (2.1) is given. Above we constructed the vector  $\mathbf{y} = (\mathbf{p}, \mathbf{x})$ , where  $\mathbf{x}$  represents the mRNA concentration and  $\mathbf{p}$  the protein concentration. According to Figure 2.2 it is natural to assume that the change in mRNA concentration  $i$  over

time is given by some function  $F$  depending on  $\mathbf{x}$  and  $\mathbf{p}$ , that is:

$$\frac{d}{dt}x_i = F_i(\mathbf{x}, \mathbf{p}) \quad (2.2)$$

Before we also assumed that there exists a fixed point  $\mathbf{y}^0$  and we stated that mRNA usually directly codes for their proteins. So, it is reasonable to assume some kind of linear relationship between the production of proteins and the perturbed mRNA concentration  $\delta\mathbf{x} = \mathbf{x} - \mathbf{x}^0$ . The associated perturbation of protein  $\alpha$  around its fixed point is then:

$$\delta p_\alpha = \sum_i C_{\alpha i} \delta x_i. \quad (2.3)$$

Where  $C_{\alpha i}$  is the interaction between mRNA molecule  $i$  and protein  $\alpha$ . Linearising around the equilibrium gives us the following equation:

$$\begin{aligned} \frac{d}{dt}\delta x_i &= \sum_j \delta x_j \frac{\partial}{\partial x_j} F_i(\mathbf{y}^0) + \sum_\alpha \delta p_\alpha \frac{\partial}{\partial p_\alpha} F_i(\mathbf{y}^0) \\ &= \sum_j \delta x_j \frac{\partial}{\partial x_j} F_i(\mathbf{y}^0) + \sum_\alpha \sum_j \frac{\partial}{\partial p_\alpha} F_i(\mathbf{y}^0) C_{\alpha j} \delta x_j \\ &= \sum_j \left( \frac{\partial}{\partial x_j} F_i(\mathbf{y}^0) + \sum_\alpha \frac{\partial}{\partial p_\alpha} F_i(\mathbf{y}^0) C_{\alpha j} \right) \delta x_j \end{aligned} \quad (2.4)$$

By rewriting the terms within the brackets as an interaction matrix  $A$  and noting that  $\delta\dot{x} = \dot{x}$ , the required equation is obtained:

$$\frac{d}{dt}x_i = \sum_j A_{ij} \delta x_j = \sum_j A_{ij} (x_j - x_j^0) \quad (2.5)$$

This is the entrywise linear differential equation (2.1), which will be used in the rest of the report. Clearly this linear model is an oversimplification of reality, it has however frequently been used recently.

It remains to define the entries from the interaction matrix. These interaction rates can be measured experimentally, to a certain extent. We wish to obtain general properties for this kind of model. It is supported experimentally, where a least-squares fit was used, that Gaussian weights for the interaction rates provide the best results (Stokić et al., 2008). In this way the interaction rates - the weight of an edge in a graph - are simulated. To fully generate a random interaction matrix a so-called Erdős–Rényi graph is constructed. This is a type of construction that determines which nodes are connected by an edge. For networks where the interaction rates are unknown, this is a common way of defining a network. Since we are working with random matrices it is also useful to make use of random matrix theory, which is further explained in chapter 3.

### 2.2.2. Erdős–Rényi Model

In graph theory the Erdős–Rényi model is a method to generate a random graph. It requires two inputs:  $n$  and  $p$ .  $n$  represents the size of the graph or the amount of nodes, while  $p$  represents the probability to create a directed edge of weight one between two nodes. In this manner the model  $G(n, p)$  constructs a graph by connecting distinct nodes at random with probability  $p$ , independent from other nodes. An example of such a graph generated by  $G(4, 0.7)$  is in Figure 2.3.

Now the interaction rates are drawn from a normal distribution with mean 0 and standard deviation 0.1, that is  $A_{ij} \sim N(0, 0.1^2)$ . For this example the interaction rates are added in Figure 2.4. Both figures result in the following adjacency matrix and interaction matrix.

$$\text{Adjacency} = \begin{bmatrix} 0 & 1 & 1 & 1 \\ 0 & 0 & 0 & 1 \\ 1 & 1 & 0 & 0 \\ 1 & 0 & 1 & 0 \end{bmatrix} \quad \text{Interaction} = \begin{bmatrix} 0 & 0 & 0.004 & 0.047 \\ -0.029 & 0 & 0.071 & 0 \\ 0.088 & 0 & 0 & -0.052 \\ -0.085 & 0.097 & 0 & 0 \end{bmatrix}$$

The adjacency matrix is created as explained in section 2.1.2, while the interaction matrix is the transpose of the adjacency matrix with the added weights. So, first the weights are added and then the transpose of the adjacency matrix is taken. To emphasize, the creation of this interaction matrix comes with two kinds of randomness: the edges in the graph and the interaction strength. The fact that the interaction matrix is the transpose of the adjacency matrix is a small detail and is due to the manner in which the differential equation 2.5 is defined. The sum is over  $j$  and the equation should be read as node  $i$  gets influenced by node  $j$ , instead of node  $i$  influences node  $j$ .

Since the matrices are generated randomly, this distinction is not necessarily required for calculations. It is only needed for understanding. For example when you want to translate the interaction matrix to a graph, or if you wish to add a directed connection yourself. Before we jump to the numerical solution of this model, we will treat some theory about random matrices.

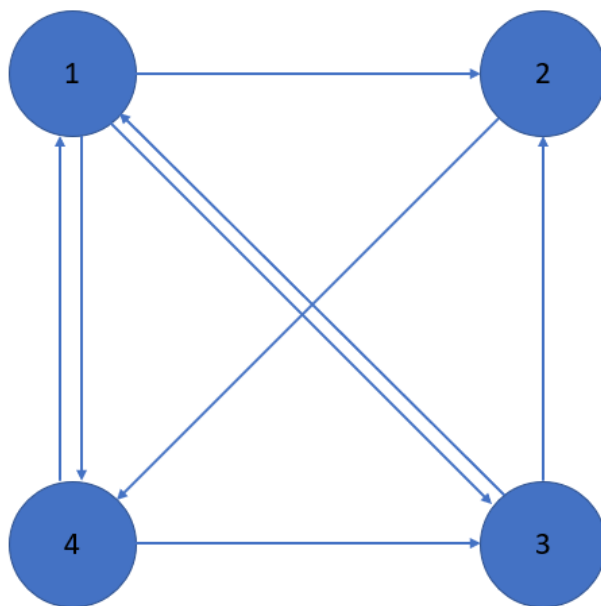


Figure 2.3: A randomly generated Erdős–Rényi graph with 4 nodes and 8 directed edges.

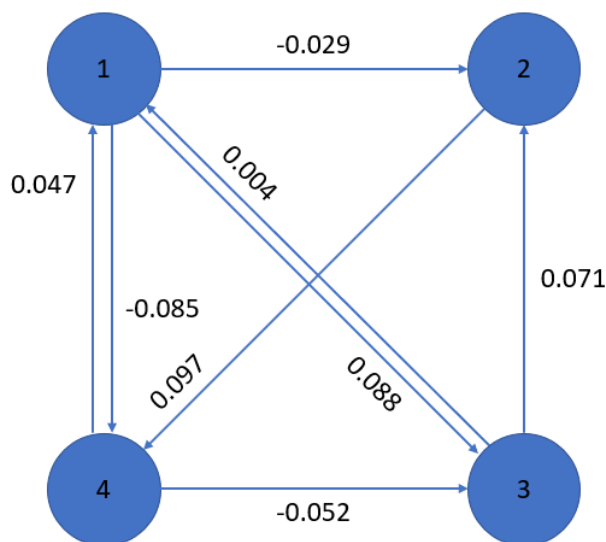


Figure 2.4: A randomly generated Erdős–Rényi graph with 4 nodes and 8 directed edges. The weights of the edges, also called the interaction rates are drawn from a normal distribution with mean 0 and standard deviation 0.1.



# 3

## Distribution of Eigenvalues: Random Matrix Theory

Eigenvalues and their corresponding eigenvectors play a crucial role in linear algebra in general and in differential equations and random matrices in particular. Normally eigenvalues of a matrix can be computed using the standard definition  $A\vec{v} = \lambda\vec{v}$ . For very small matrices this can be done analytically, however for larger matrices this becomes impossible. A numerical estimation of eigenvalues is then an option. There is a lot of theory about the eigenvalues of random matrices. In this chapter we introduce some aspects of random matrix theory that we will later use to examine the properties of solutions of equation 2.1.

In subsection 3.1 Wigner's semicircle law is introduced and proofed for real symmetric matrices, this law predicts the distribution of the real part of the eigenvalues of a random matrix. In subsection 3.2 Girko's law is introduced, also known as the circular law. This law states that the eigenvalues of a random matrix are distributed uniformly on a disk in the complex plane  $\mathbb{C}$ . Of course both laws only hold under certain circumstances.

### 3.1. Wigner's Semicircle Law

In this section the very important semicircle law in random matrix theory is stated and proved. This law is as important to random matrix theory as the central limit theorem is to probability theory. First we will give the definition of a Wigner matrix and we will quote the Wigner's semicircle law. After that the Wigner's semicircle law is proved by using the Stieltjes transform method, also known as the Cauchy transformation.

**Definition 3.1.1** (Real Wigner matrix). A real Wigner matrix  $M$  is a real valued symmetric matrix where the upper-triangular entries  $M_{ij}$ , with  $i > j$  are iid Gaussian random variables with mean zero and variance  $\frac{\sigma^2}{N}$ . The diagonal entries  $M_{ii}$  are iid Gaussian random variables, independent from the off-diagonal entries, with mean 0 and variance  $\frac{2\sigma^2}{N}$ . In literature this choice of matrix is also called the Gaussian orthogonal ensemble.

**Definition 3.1.2** (Empirical spectral distribution). For any square matrix  $A$ , the probability distribution  $P$  which puts equal mass on each eigenvalue of  $A$  is called the Empirical Spectral Distribution or measure (ESD) of  $A$ . (Bose et al., 2003)

This says that if  $\lambda$  is an eigenvalue of an  $N \times N$  matrix  $A_N$  with multiplicity  $m$ , then the ESD puts a mass of  $\frac{m}{N}$  at  $\lambda$ .

**Theorem 3.1.1** (Wigner's semicircle law). Let  $\{M_n\}_{n=1}^{\infty}$  be a sequence of Wigner matrices. Then the empirical spectral distributions (ESDs)  $\mu_{M_n}$  converge almost surely to the Wigner semicircle distribution:

$$\mu_{sc} := \frac{1}{2\pi\sigma^2} \sqrt{4\sigma^2 - x^2} \mathbb{1}_{|x| \leq 2\sigma} \quad (3.1)$$

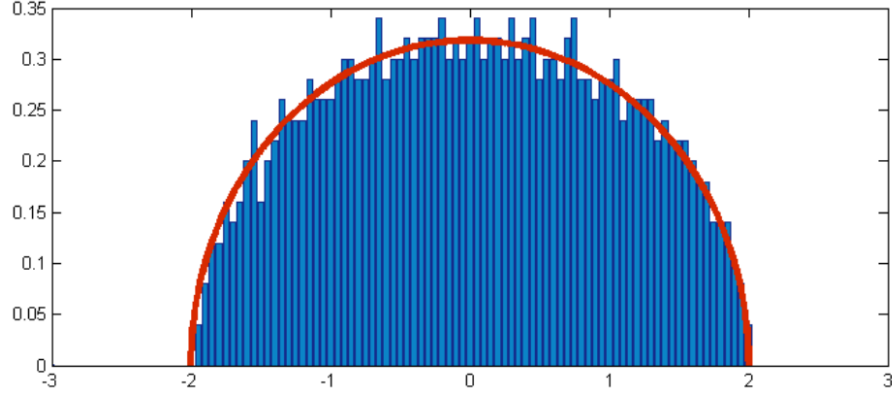


Figure 3.1: Illustration of Wigner's semicircle in action: "Simulation of the semicircle law using 1000 samples of the eigenvalues of 1000 by 1000 matrices. Bin size is 0.05" (Feier, 2012)

It essentially states that the (real part) eigenvalues of a real Wigner matrix are distributed in a semicircle with center 0 and radius 2. In Figure 3.1 this is illustrated.

*Proof.* In this part we will proof Wigner's semicircle law Theorem 3.1.1 by using the Stieltjes transformation method. This will give us information about all the moments of a random matrix and also about the density of its eigenvalues in the large limit  $N$ . Given an  $N \times N$  real Wigner matrix  $A$ , with  $A = M_N$ . In this way the index  $N$  is dropped if the dimension is known - then its resolvent is given by

$$G_A(z) = (z\mathbf{I} - A)^{-1} \quad (3.2)$$

Where  $z$  is a complex variable defined away from all the (real) eigenvalues of  $A$  and  $\mathbf{I}$  denotes the identity matrix. Then the Stieltjes transform of  $A$  as  $N$  goes to  $\infty$  is given by

$$g_N^A = \frac{1}{N} \text{Tr}(G_A(z)) = \frac{1}{N} \sum_{k=1}^N \frac{1}{z - \lambda_k} \quad (3.3)$$

Here  $\text{Tr}$  is the trace operator, which is the sum of the diagonal elements. This is equal to the RHS of equation 3.3, by using two facts: 1) the trace is equal to the sum of eigenvalues and 2) if  $\lambda$  is an eigenvalue from  $B$ , then  $\frac{1}{\lambda}$  is an eigenvalue from  $B^{-1}$ . The  $\lambda_k$  are the eigenvalues of the matrix  $A$ .

Now let us define the empirical spectral distribution (ESD) for a given random matrix  $A$ :

$$\rho_N(\lambda) = \frac{1}{N} \sum_{k=1}^N \delta(\lambda - \lambda_k) \quad (3.4)$$

Here  $\delta(x)$  is the Dirac delta function. Then the exact formula for the Stieltjes transform can be written as

$$g_N^A = \int_{-\infty}^{\infty} \frac{\rho_N(\lambda)}{z - \lambda} d\lambda \quad (3.5)$$

Note that  $g_N^A(z)$  is well defined for any  $z \notin \lambda_k : 1 \leq k \leq N$ . Plugging in equation 3.4 and using the integral rules for the Dirac delta function  $\delta(x)$

$$g_N^A = \int_{-\infty}^{\infty} \frac{1}{N} \sum_{k=1}^N \frac{\delta(\lambda - \lambda_k)}{z - \lambda} d\lambda = \frac{1}{N} \sum_{k=1}^N \frac{1}{z - \lambda_k} \quad (3.6)$$

Where the RHS is exactly the same as the RHS from equation 3.3. On the other hand, the Stieltjes transform can be written as Taylor series around 0 by using the geometric series of  $\frac{1}{N} \sum_{k=1}^N \frac{1}{z - \lambda_k}$ , for

the full derivation see Appendix A (P.51)

$$\frac{1}{N} \sum_{k=1}^N \frac{1}{z - \lambda_k} = \sum_{k=0}^{\infty} \frac{1}{z^{k+1}} \frac{1}{N} \text{Tr}(A^k) \quad (3.7)$$

$$\frac{1}{N} \text{Tr}(A^0) = \frac{1}{N} \text{Tr}(\mathbf{I}) = 1$$

Which is well behaved for  $z \rightarrow \infty$ .

It is known (by the Borel-Cantelli lemma) that for any  $z$  large enough,  $g_N^A(z) - \mathbb{E}g_N^A(z)$  converges almost surely to zero (Tao, 2010). We then expect that for large enough  $z$ , the function  $g_N^A(z)$  converges to a deterministic limit  $g(z)$ , where  $g(z) = \lim_{N \rightarrow \infty} \mathbb{E}[g_N^A(z)]$ . So  $g_N^A(z)$  is close to its mean, but  $\mathbb{E}g_N^A(z)$  is still unknown.

$$\begin{aligned} \mathbb{E}g_N(z) &= \mathbb{E} \frac{1}{N} \text{Tr}(z\mathbf{I} - A)^{-1} \\ &= \frac{1}{N} \mathbb{E} \sum_{j=1}^N [(z\mathbf{I} - A)^{-1}]_{jj} \\ &= \frac{1}{N} \sum_{j=1}^N \mathbb{E} [(z\mathbf{I} - A)^{-1}]_{jj} \end{aligned} \quad (3.8)$$

Where  $[B]_{jj}$  denotes the  $jj$  component, or simply the diagonal elements, of a matrix  $B$ . The last equality holds because of the linearity of the trace. Since  $A$  is a Wigner matrix, the random variables  $[(z\mathbf{I} - A)^{-1}]_{jj}$  have the same distribution (Tao, 2010), which implies that the expectation of those random variables are the same. Equation 3.8 then reduces to

$$\mathbb{E}g_N^A(z) = \mathbb{E} [(z\mathbf{I} - A)^{-1}]_{11} \quad (3.9)$$

In this way we only have to compute the first entry of the resolvent  $G_A(z) = (z\mathbf{I} - A)^{-1}$ . To calculate this entry of the inverse, we shall use the Schur complement.

**Definition 3.1.3** (Schur complement). Given that matrix  $H$  of size  $N \times N$  and  $D$  are invertible and that  $H$  is given by

$$H = \begin{bmatrix} A & B \\ C & D \end{bmatrix}$$

Where  $A = n \times n$ ,  $B = n \times (N - n)$ ,  $C = (N - n) \times n$  and  $D = (N - n) \times (N - n)$ . Then the inverse  $H^{-1}$  is given by

$$H^{-1} = Q = \begin{bmatrix} Q_{11} & Q_{12} \\ Q_{21} & Q_{22} \end{bmatrix}$$

The upper left  $n \times n$  block of  $Q$  is given by  $(Q_{11})^{-1} = A - B(D)^{-1}C$ . The other blocks can also be computed, but we are only interested in the upper left block.

This will be used to compute the inverse of  $M = (z\mathbf{I} - A)$ , where we will introduce the following notation

$$M = (z\mathbf{I} - A) = \begin{bmatrix} M_{11} & M_{12} \\ M_{21} & m \end{bmatrix}$$

Here  $M_{11}$  is the first entry of matrix  $M$ ,  $M_{21}$  is the first column of  $M$  without the entry  $M_{11}$  and  $M_{12}$  is the first row of  $M$  without the entry  $M_{11}$ , both of size  $N - 1$ . So,  $m$  is the submatrix of  $M$  of size  $(N - 1) \times (N - 1)$ , with the first row and column removed. Then, by applying the Schur complement with  $A = M_{11}$ ,  $B = M_{12}$ ,  $C = M_{21}$  and  $D = m$  we obtain the first 'block' of the inverse, which is a deterministic  $1 \times 1$  'matrix', so the reciprocal is defined.

$$\frac{1}{[(z\mathbf{I} - A)^{-1}]_{11}} = M_{11} - M_{12}(m)^{-1}M_{21} = M_{11} - \sum_{k,l=1}^{N-1} [M_{12}]_{1k} [(m)^{-1}]_{kl} [M_{21}]_{l1} \quad (3.10)$$

Where  $[M_{12}]_{1k}$ ,  $[(m^{-1})]_{kl}$  and  $[M_{21}]_{l1}$  are the entries of  $[M_{12}]$ ,  $m^{-1}$  and  $M_{21}$  respectively. If we take the expectation of both sides this expression turns into

$$\mathbb{E} \frac{1}{[(z\mathbf{I} - A)^{-1}]_{11}} = \mathbb{E}(M_{11}) - \sum_{k,l=1}^{N-1} [M_{12}]_{1k} [m^{-1}]_{kl} [M_{21}]_{l1} \quad (3.11)$$

Recall that the  $[M_{12}]_{1k}$  were iid random variables with mean 0 and variance  $\frac{\sigma^2}{N}$ , the same holds for  $[M_{21}]_{l1}$  due to symmetry (definition Wigner matrix 3.1.1). Also, note that  $M_{12}$  and  $m$  are therefore independent. So, using the linearity and independence properties of expectation (Appendix A, P.52), this reduces to

$$\mathbb{E} \frac{1}{[(z\mathbf{I} - A)^{-1}]_{11}} = \mathbb{E}(M_{11}) - \mathbb{E} \left( \sum_{k,l=1}^{N-1} [M_{12}]_{1k} [m^{-1}]_{kl} [M_{21}]_{l1} \right) = \mathbb{E}(M_{11}) - \frac{\sigma^2}{N} \cdot \mathbb{E} \text{Tr}(m^{-1}) \quad (3.12)$$

First we notice that the expectation of  $M_{11}$  is  $z$ , as the diagonal elements  $A_{ii}$  have mean 0. Next, we notice that  $\frac{1}{N} \text{Tr}[m^{-1}]$  is approximately the Stieltjes transform of a Wigner matrix of size  $N - 1$ . In the large  $N$  limit, the idea is that the Stieltjes transformation of a Wigner matrix of size  $N$  and size  $N - 1$  converges to the same Stieltjes transformation. Intuitively it might be clear that the spectral properties of matrix  $A$  and  $A_{N-1}$  should be approximately the same:

$$\frac{1}{N} \text{Tr}((z\mathbf{I} - A)^{-1}) \approx \frac{1}{N-1} \text{Tr}((z\mathbf{I}_{N-1} - A_{N-1})^{-1}) \quad (3.13)$$

So, the Stieltjes transformation is stable for large  $N$ . Therefore,

$$\mathbb{E} \frac{1}{N} \text{Tr}(m^{-1}) \rightarrow g(z) \quad (3.14)$$

We will also use the stability of the Stieltjes transformation to argue that

$$\mathbb{E} \frac{1}{[(z\mathbf{I} - A)^{-1}]_{11}} = \frac{1}{\mathbb{E} [(z\mathbf{I} - A)^{-1}]_{11}} \quad (3.15)$$

Normally this does not hold. But it is allowed if  $[(z\mathbf{I} - A)^{-1}]_{11}$  is close to a deterministic number without variance, which we assume for large  $N$ . Combining above result with equation 3.9 we then have

$$\mathbb{E} \frac{1}{[(z\mathbf{I} - A)^{-1}]_{11}} = \frac{1}{\mathbb{E} [(z\mathbf{I} - A)^{-1}]_{11}} = \frac{1}{\mathbb{E} g_N^A(z)} \rightarrow \frac{1}{g(z)} \quad (3.16)$$

Putting all our results into equation 3.12 we obtain the following remarkable equation:

$$\frac{1}{g(z)} = z - \sigma^2 g(z) \quad (3.17)$$

Solving this equation for  $g(z)$ , we get

$$\sigma^2 g^2 - zg + 1 = 0 \rightarrow g(z) = \frac{z \pm \sqrt{z^2 - 4\sigma^2}}{2\sigma^2} \quad (3.18)$$

Now we should take the correct sign for large  $z$ . The (+) sign gives that  $g(z) \sim z$ , which diverges and is therefore incorrect, since  $g(z)$  was well behaved for  $z \rightarrow \infty$ . So, we should take the (-) sign such that  $g(z) \sim \frac{1}{z}$  (Appendix A, P.53).

$$g(z) = \frac{z - \sqrt{z^2 - 4\sigma^2}}{2\sigma^2} \quad (3.19)$$

Now that we have found  $g(z)$ , we wish to recover the ESD  $\rho_N(\lambda)$  from equation 3.5. To understand this part either some topology knowledge is required (Tao, 2010) or some (advanced) complex analysis (Potters and Bouchaud, 2020). Sadly, this is beyond my knowledge. Nevertheless, we can use the

given results. If you are interested in the details I wish to refer you to above references.

The following result is given: Stieltjes inversion formula

$$\lim_{\eta \rightarrow 0^+} \text{Im } g(x - i\eta) = \pi \rho(x) \quad (3.20)$$

Where  $\rho(x)$  is the ESD. Then combining equation 3.19 with the Stieltjes inversion formula, we get

$$\begin{aligned} \lim_{\eta \rightarrow 0^+} \text{Im } \frac{g(x - i\eta)}{\pi} &= \lim_{\eta \rightarrow 0^+} \text{Im } \frac{(x - i\eta) - \sqrt{(x - i\eta)^2 - 4\sigma^2}}{2\pi\sigma^2} \\ &= \text{Im } \frac{x - \sqrt{x^2 - 4\sigma^2}}{2\pi\sigma^2} \\ &= \frac{\sqrt{4\sigma^2 - x^2}}{2\pi\sigma^2} = \rho(x) \end{aligned} \quad (3.21)$$

Where  $g(z)$  only has an imaginary part if  $(x^2 - 4\sigma^2) < 0$ , so  $-2\sigma \leq x \leq 2\sigma$ , which is why we switch the place of  $x^2$  and  $4\sigma^2$  in the last equality. Hence we have finally arrived at the result from Wigner's semicircle law Theorem 3.1.1

$$\rho(x) = \frac{\sqrt{4\sigma^2 - x^2}}{2\pi\sigma^2} \mathbb{1}_{|x| \leq 2\sigma} \quad (3.22)$$

□

The idea of this proof is based on A first course in Random Matrix Theory by Potter. Some details were added and omitted, to create a understandable proof for bachelor math students. The idea of the added details were found in Tao, 2010 or Feier, 2012.

## 3.2. Girko's Law

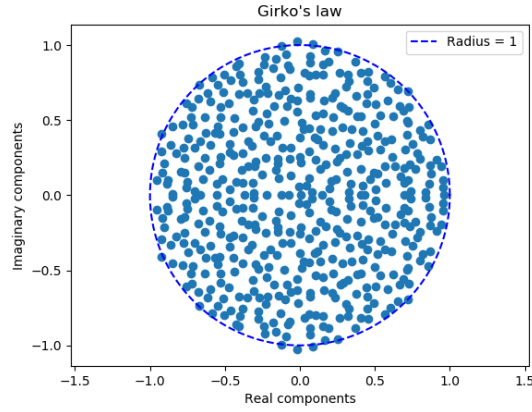
Another law in random matrix theory is Girko's law, also known as the circular law. This law holds for many random matrices in general. We are interested in a random matrix where the off-diagonal entries are taken from a normal distribution.

**Theorem 3.2.1** (Girko's law). Let  $A$  be a random matrix of size  $n \times n$  with main diagonal entries 0 and off-diagonal entries taken from a normal distribution with mean 0 and variance  $\sigma_A^2$ , that is  $A_{ii} = 0$  and  $A_{ij} \sim (N(0, \sigma_A^2))$ . Then the eigenvalues of matrix  $A$ , in the large limit  $n$ , are uniformly distributed on a circle in the complex plane with center  $\mathbf{0}$  and radius  $\rho = \sigma_A \sqrt{\langle k \rangle}$  (Stokić et al., 2008). Where  $\langle k \rangle$  is the average connectivity.

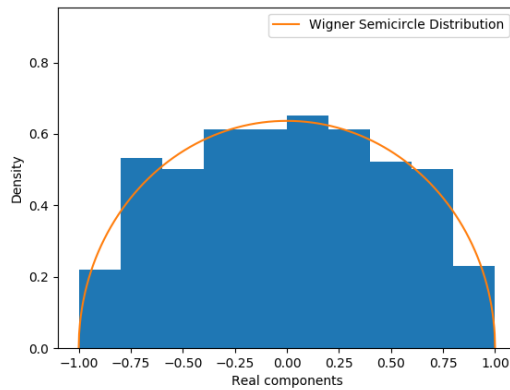
This is a powerful law which can be used to predict the distribution of the eigenvalues of a random matrix  $A$ . In particular it can be used to predict the largest eigenvalue of a matrix, which plays a major role in the stability of a system. For this see chapter 4. A proof of this law is beyond the scope of this paper, but was done recently by Terence Tao et al. in 2010.

In the next two subsections we will explore the center and radius of Girko's circle. But first an illustration of Girko's law in action: Figure 3.2a. For this example we plotted the eigenvalue distribution of a fully connected - apart from the diagonal which remains 0 for now - random matrix  $A$  of size  $n = 500$  and with edge probability  $p = 1$ . The entries are taken from a  $N(0, \frac{1}{\sqrt{n}})$  distribution, such that the eigenvalues are distributed on a unit complex circle.

It is noteworthy that the real parts of all the eigenvalues are distributed on Wigner's semicircle, see Figure 3.2b. Since the network consists of 'only' 500 nodes, the distribution of the eigenvalues is not spot on.



(a) Girko's law



(b) Wigner's Semicircle

Figure 3.2: (a) The distribution of the eigenvalues on the unit complex circle according to Girko's Law. (b) The distribution of the real parts of the eigenvalues on the domain  $[-1, 1]$ . There is a more general distribution for the Wigner Semicircle, namely  $\rho(x) = \frac{2\sqrt{R^2 - x^2}}{\pi R^2}$ . Where the  $x$ -axis is then  $[-R, R]$ . In this case we have  $R = 1$ , this radius should agree with the radius of Girko's circle.

### 3.2.1. Center

What would happen to the eigenvalue distribution of the matrix  $A$ , if the diagonal elements of weight  $W$  are added? It is known that the eigenvalues of our random matrix  $A$  are uniformly distributed in the complex circle around the origin with radius  $r$ . Adding the diagonal elements such that  $H = (A - W\mathbf{I})$ , where  $\mathbf{I}$  is the identity matrix, shifts the center of the circle to  $-W$ . A simple proof of this is as follows: Given is that  $A\vec{v}_i = \lambda_i\vec{v}_i$ , with  $\lambda_i$  distributed according to Girko's law. Then

$$(A - W\mathbf{I})\vec{v}_i = A\vec{v}_i - W\mathbf{I}\vec{v}_i = \lambda_i\vec{v}_i - W\vec{v}_i = (\lambda_i - W)\vec{v}_i$$

So the matrix  $H$  with diagonal elements has eigenvalues of matrix  $A$  shifted by  $-W$ . The eigenvectors however, remain the same. Which implies that Girko's circle simply shifts along with center  $(-W, 0)$ . In figure 3.3 the shifted circle for  $W = 2$  is illustrated.

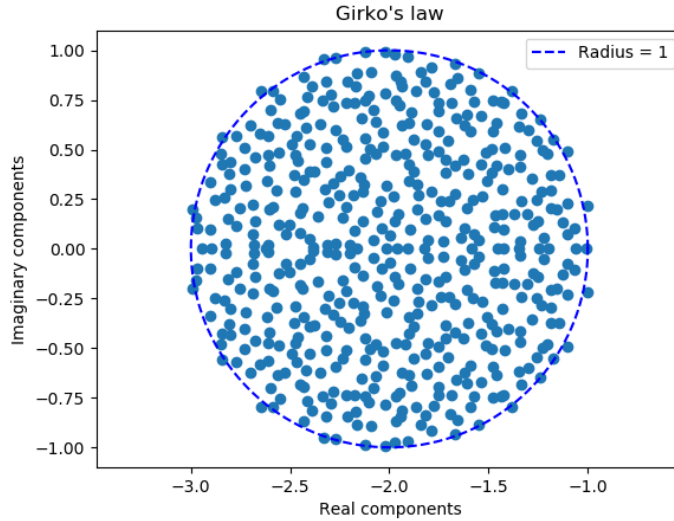


Figure 3.3: Shifted Girko's Law for network size  $n=500$ , edge probability  $p=1$  and diagonal elements  $W=2$ . The center of Girko's circle shifts to  $-2$ , due to the diagonal elements  $W=2$ . The off diagonal entries are taken from a  $N(0, \frac{1}{\sqrt{n}})$  distribution, to obtain a unit complex circle.

### 3.2.2. Radius

It is known that the radius of the complex circle is given by  $\rho = \sigma\sqrt{\langle k \rangle}$ . Here  $\sigma$  is the square root of the variance  $\sigma^2$ , also called the standard deviation.  $\sqrt{\langle k \rangle} = \frac{L}{n}$  is the average connectivity, where  $L$  was the amount of edges, or the amount of non-zero entries in a matrix  $A$ , and  $N$  the amount of nodes, or the size of the network (see subsection 2.1.2).

This implies that there are two ways to change the radius of the complex circle. You can adjust the variance or the average connectivity. The first is done by simply taking the interaction rates from a different normal distribution with mean 0 and variance  $\sigma^2$ . This is illustrated in Figure 3.4.

The second, changing the average connectivity  $\sqrt{\langle k \rangle}$  for a certain size  $n$ , can be done by adjusting the edge probability  $p$ . This is illustrated in Figure 3.5. The expected average connectivity depending on the edge probability  $p$  and size  $n$ , is approximately  $np$ . This is due to the fact that there are  $n^2$  entries in an adjacency matrix  $A$ , where each entry has probability  $p$  to be non-zero. Then the total amount of non-zero entries is a binomial distribution  $\text{Bin}(n^2, p)$ , which has expectation  $n^2p$ . Putting this into the definition of  $\sqrt{\langle k \rangle} = \frac{L}{n} = \frac{n^2p}{n} = np$  gives our result.

The most important part is that the radius of the complex circle gives an estimation of the largest real part of all eigenvalues, also called the maximal Lyapunov exponent (MLE). The variance of the interaction rates for a specific network of genes does not change, so  $\sigma$  can be considered constant. Then the radius  $\rho$  only depends on the average connectivity  $\langle k \rangle$ , that is

$$\rho(\langle k \rangle) = \sigma\sqrt{\langle k \rangle}. \quad (3.23)$$

Then the MLE for a sufficiently large matrix  $A$ , such that Girko's law holds, is approximately  $\sigma\sqrt{\langle k \rangle}$ .

Now, let us define a new weight  $D$ , which is scaled in a special way:

$$D = \frac{W}{\sigma} \quad (3.24)$$

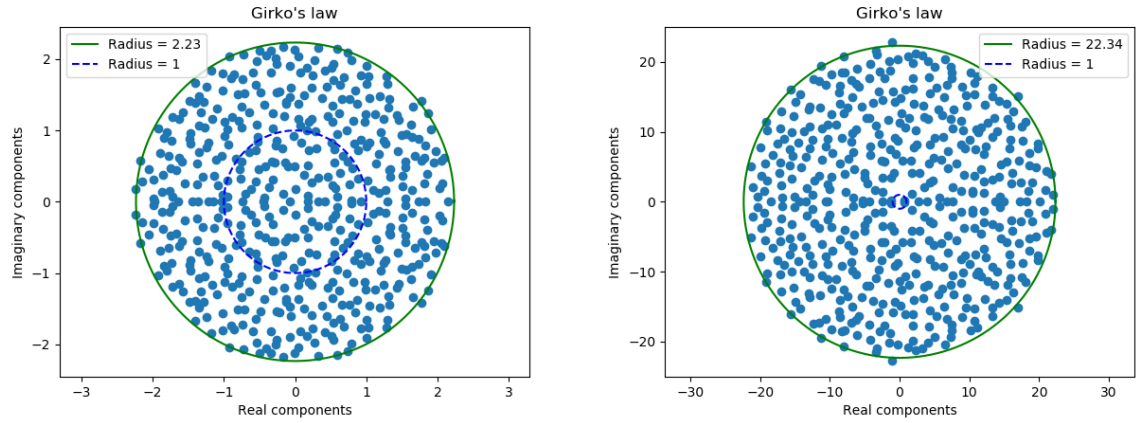
Without loss of generality we can set  $\sigma = 0.1$  for the rest of the report, unless stated otherwise, as it is just a scaling of weights. Adding the diagonal elements  $W$ , such that  $H = (A - W\mathbf{I})$ , changes the center of our circle to  $(-W, 0)$ , which was found in subsection 3.2.1. So the MLE for matrix  $H$  is approximately  $\sigma\sqrt{\langle k \rangle} - W$ . Writing this in terms of  $D$ :

$$\sigma\sqrt{\langle k \rangle} - W = \sigma(\sqrt{\langle k \rangle} - D) \quad (3.25)$$

Gives us another approximation for the MLE:

$$MLE \approx \sigma(\sqrt{\langle k \rangle} - D). \tag{3.26}$$

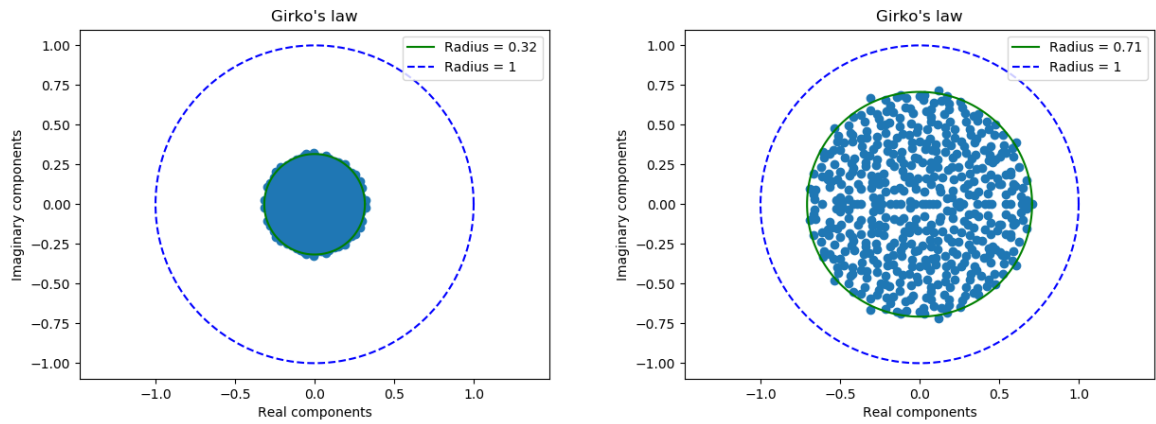
This is an important result which is needed for the non-linear model in Chapter 5. But, before we study the non-linear model we will explore the linear model first.



(a)  $\sigma = 0.1$

(b)  $\sigma = 1$

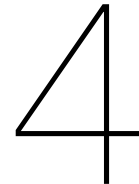
Figure 3.4: Radius of Girko's circle for different values of  $\sigma$ , while the edge probability  $p = 1$ , and so the average connectivity  $\langle k \rangle$  is constant. The dotted blue circle is the unit circle for comparison. The network size is  $n = 500$ .



(a)  $p = 0.1$  and  $\langle k \rangle = 50$

(b)  $p = 0.5$  and  $\langle k \rangle = 250$

Figure 3.5: Radius of Girko's circle for different values of the average connectivity  $\langle k \rangle$ , while  $\sigma = \frac{1}{\sqrt{500}}$ . The dotted blue circle is the unit circle for comparison. The network size is  $n = 500$ .



# Linear Model for Gene Networks

In this chapter the properties of the following linear model are discussed:

$$\dot{\mathbf{x}} = A(\mathbf{x} - \mathbf{x}^0) \quad (4.1)$$

Here  $A$  is the interaction matrix and  $\mathbf{x}^0$  is the stationary point. Perturbations about this stationary point  $\delta\mathbf{x} = \mathbf{x} - \mathbf{x}^0$  then satisfy the following differential equation, which is a more convenient notation.

$$\delta\dot{\mathbf{x}} = A\delta\mathbf{x} \quad (4.2)$$

Using this linear model we are interested in how different organisms interact. Typically we think of organisms like bacteria or fungi such as *E. Coli* or *S. Cerevisiae* respectively. To that end we study the eigenvalues of random interaction matrices that have a block structure. Each block can then be envisioned to model a certain gene pool that corresponds to an organism. An example of a gene pool of *S. Cerevisiae*, also known as yeast, is given in Figure 4.1.

When organisms interact, some of the genes of one organism can influence the expression of genes of another organism. This is because the expression of genes depend on the presence of the corresponding proteins, and so on the concentration of mRNA. It is interesting how these interactions affect the stability of the organism its gene network, that is, how the interactions reflect themselves in the distribution of eigenvalues of the corresponding interaction matrix. Such an interaction can be modelled by adding an edge between the networks, also called an “interconnection”. This will soon become clear in subsection 4.3

In the upcoming chapter, first the general solution to equation 4.2 and its stability is discussed (4.1). Then we study a simple block matrix without an interconnection in subsection 4.2. In subsection 4.3 the networks are connected by an edge between the different blocks, an interconnection. Finally, we will check some special cases of a positive and negative interaction matrix in subsections 4.4 and 4.5 respectively.

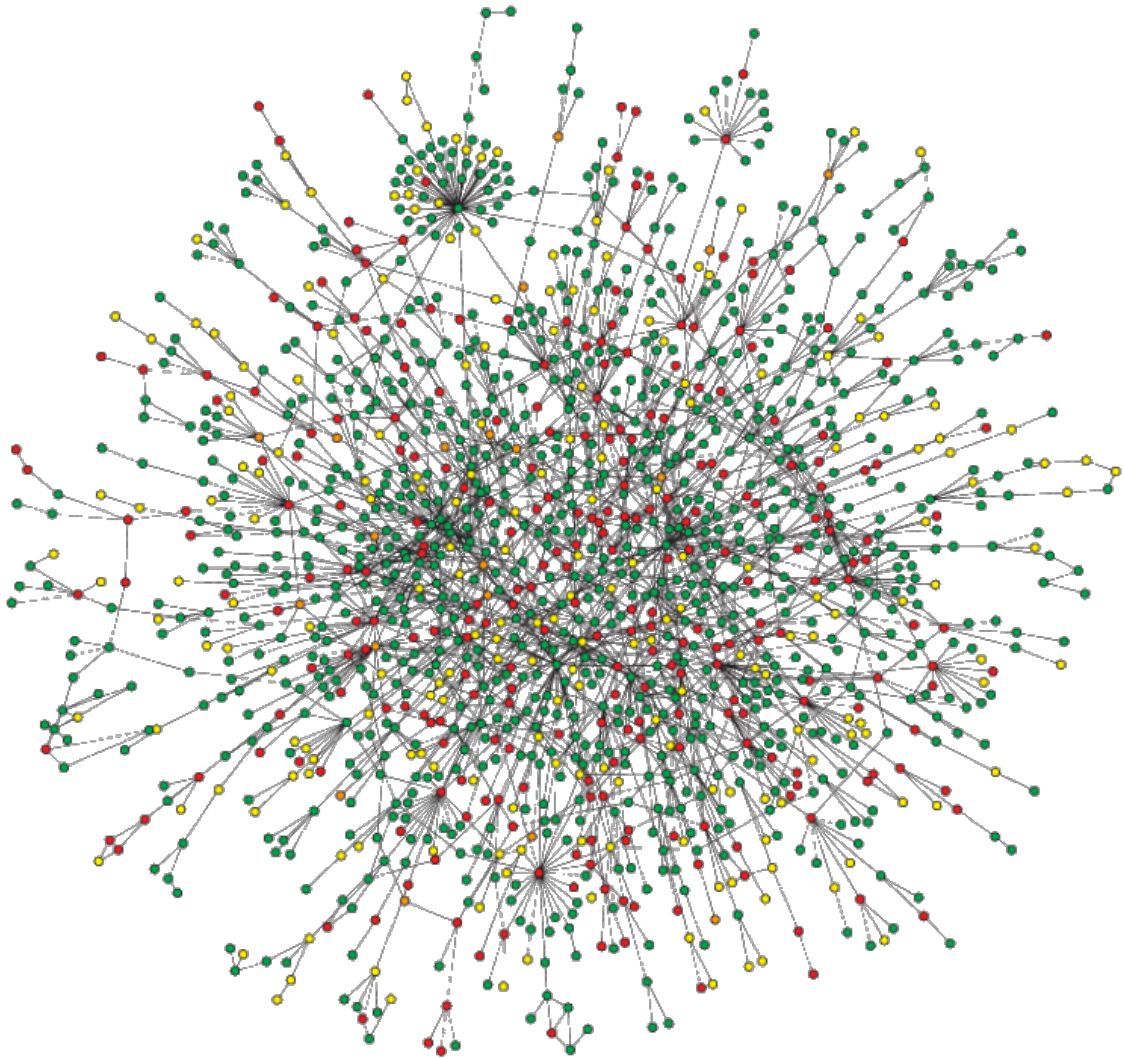


Figure 4.1: An example of the gene network of Baker's yeast. It consists of 1870 proteins as nodes connected by 2240 identified direct physical interactions, directed edges. Such a graph can be translated to an interaction matrix. "Map of protein-protein interactions. The largest cluster, which contains 78% of all proteins is shown. The color of a node signifies the phenotypic effect of removing the corresponding protein (red=lethal, green=non-lethal, orange=slow growth, yellow=unknown)" (Jeong et al., 2001)

## 4.1. Stability of Solutions

In general, if the interaction matrix  $A$  is diagonalisable, the solution to equation 4.2 is given by equation 4.3. Here  $C$  is a column vector of size  $n$ , which contains the coefficients to solve an initial-value problem, with initial condition  $\mathbf{x}_0$ .

$$\delta \mathbf{x} = e^{At} C = c_1 \mathbf{v}_1 e^{\lambda_1 t} + c_2 \mathbf{v}_2 e^{\lambda_2 t} + \dots + c_n \mathbf{v}_n e^{\lambda_n t} \quad (4.3)$$

We are interested in the stability of the solution to equation 4.2. Is the solution unstable, stable or asymptotically stable? These are also classified as divergent, oscillatory and convergent respectively. The stability of the solution is directly determined by the eigenvalues of matrix  $A$ . A solution is unstable if at least one eigenvalue of  $A$  has positive real part. The solution is asymptotically stable if all the eigenvalues of  $A$  have negative real part. The solution is stable if there is an eigenvalue that has real part zero and a zero or non-zero imaginary part. For the latter, it should be noted that the algebraic multiplicity of the eigenvalue should be equal to the geometric multiplicity for stability. In the figure below these types of behaviour are visualised:

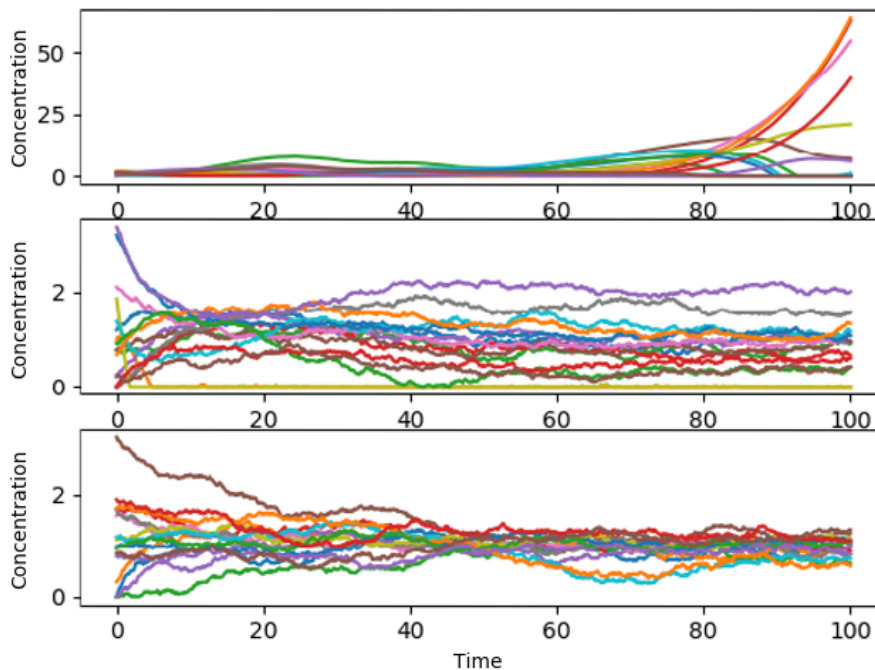


Figure 4.2: Visualisation of different types of stability. The first graph shows divergent behaviour, the solution shows big deviations from the equilibrium. The second graph shows oscillatory behaviour, the solution oscillates around the equilibrium  $\mathbf{x}^0$ . The last graph shows convergent behaviour, the solution tends to grow towards the equilibrium  $\mathbf{x}^0$ . Figure adapted from (Sanders, 2020)

## 4.2. Independent Networks

In this section we shall investigate the case that the interaction matrix  $A$  consists of two independent networks. So,  $A$  is a block diagonal matrix of the form:  $\begin{bmatrix} A_1 & 0 \\ 0 & A_2 \end{bmatrix}$ . We restrict ourselves to two independent networks, but this can be extended to three, or more generally  $n$  independent networks. Similar results hold for the larger systems.

In Linear Algebra there is a well-known theorem to determine the eigenvalues of a block diagonally structured matrix. It simply says that the eigenvalues of the whole matrix  $A$ , is equal to the union of the eigenvalues of the matrices  $A_1$  and  $A_2$ . The eigenvectors are now of the form  $\begin{bmatrix} v_i \\ 0 \end{bmatrix}$  and  $\begin{bmatrix} 0 \\ w_i \end{bmatrix}$ , where  $v_i$  and  $w_i$  are the eigenvectors of  $A_1$  and  $A_2$  respectively. So, only their dimension should be extended by some zeros to fit the size of the network. Therefore, using equation 4.3, the stability and the solution remains the same. As expected, the networks do not interact in any way and they simply continue their way of living as if the other network does not exist.

For the upcoming examples two fully connected networks, each consisting of 4 mRNA molecules, are used. The equilibrium  $\mathbf{x}^0$  is chosen as  $\mathbf{x}^0 = 10^3$ . The entries of  $A_1$  and  $A_2$  are randomly generated via a  $N(0, \frac{1}{4})$  distribution. A normal distribution with mean 0 and variance  $\frac{1}{4}$ . For convenience the entries are rounded off to 2 decimals. The diagonal elements  $W$  are chosen as 0.4, unless stated otherwise. Since the assumption is that each node has an inhibitory effect on itself, also a minus sign (-) is required on the diagonal. The following block matrices  $A_1$  and  $A_2$  were generated.

$$A_1 = \begin{bmatrix} -W & -0.38 & 0.74 & -0.12 \\ -0.22 & -W & 0.34 & -0.16 \\ -0.44 & 0.21 & -W & -0.10 \\ 1.93 & 0.60 & 0.22 & -W \end{bmatrix}$$

$$A_2 = \begin{bmatrix} -W & -0.16 & 1.10 & -0.08 \\ 0.11 & -W & 0.89 & -0.36 \\ -0.54 & 0.24 & -W & 0.43 \\ 0.18 & 0.44 & 0.74 & -W \end{bmatrix}$$

Each matrix has 4 eigenvalues which are plotted in the unit circle with center  $(-0.4, 0)$  in Figure 4.3. The eigenvalues are also written down and rounded off to 2 decimals for convenience. For  $A_1$  the eigenvalues are:

$$\lambda_{0,1} = -0.38 \pm 0.69i \quad \lambda_{2,3} = -0.42 \pm 0.19i$$

While  $A_2$  has the following eigenvalues:

$$\lambda_{4,5} = -0.76 \pm 0.70i \quad \lambda_{6,7} = -0.038 \pm 0.16i$$

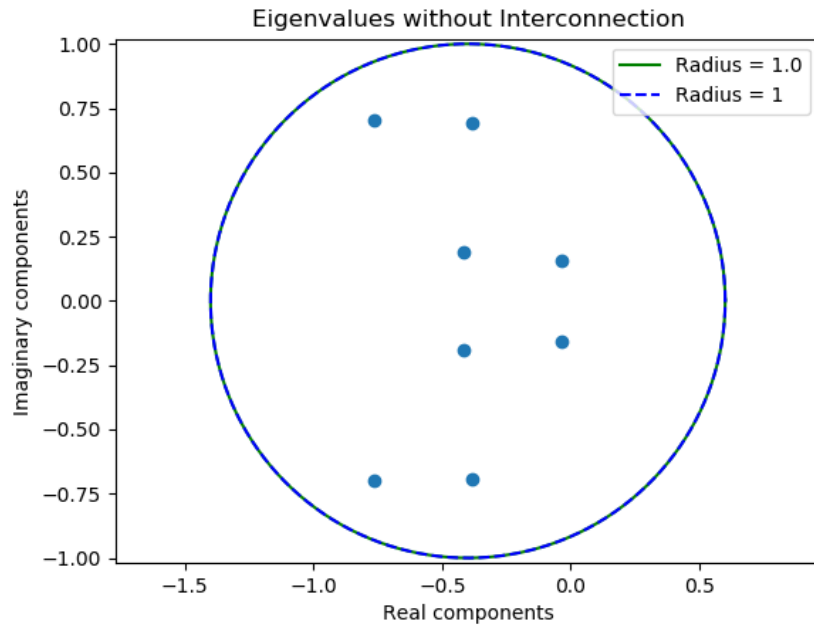


Figure 4.3: Eigenvalue distribution of two independent networks consisting of 4 nodes each. The blue dotted line represents the unit complex circle. The green line is the expected radius according to Girko's law. In this case these two coincides due to the choice of  $\sigma^2 = \frac{1}{4}$  and edge probability  $p = 1$

In this case each eigenvalue has a negative real part. Our solution is therefore asymptotically stable. So, it is expected that the solution converges to its equilibrium  $\mathbf{x}^0 = 10^3$ . The speed of convergence depends on the magnitude of the negative real part. This is due to the fact that  $e^{\lambda_i t}$  (equation 4.3) goes to zero faster if  $\lambda_i$  is more negative.

With this in mind, the numerical solution is plotted in Figure 4.4. The initial concentration  $\mathbf{x}_0$  of all mRNA concentrations is chosen as  $\mathbf{x}_0 = 1001$ . Indeed the solution is asymptotically stable. Also, since the real part of  $\lambda_{6,7}$  is close to zero ( $\text{Re}(\lambda_{6,7}) = -0.038$ ), the second network ( $A_2$ ) consisting of the nodes  $X_4, X_5, X_6$  and  $X_7$  converges less quickly than network  $A_1$ .

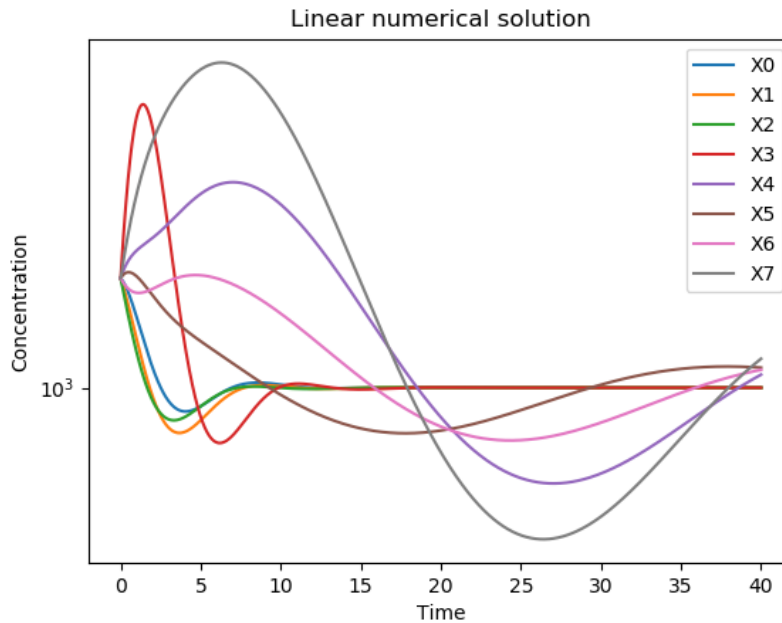


Figure 4.4: Numerical solution for the linear model of two independent networks. The mRNA concentration  $\mathbf{x}$  is plotted vs time. Network 1 consists of the nodes  $X_0$  up to  $X_3$  and network 2 consists of the nodes  $X_4$  up to  $X_7$ . Both solutions are asymptotically stable, where network 1 converges faster than network 2.

#### 4.2.1. Note on the Numerical Solution

In this small subsection the numerical method to generate the numerical solutions is described. In theory the linear model could be solved analytically by using the matrix exponential. Also the solution to the non-linear model could possibly be solved analytically by using the Fokker-Planck equations. We are however mostly interested in the stability of the solution, a numerical method is then sufficient.

In the rest of the report we shall use the forward Euler method, which is a first-order method, to generate the numerical solutions. The time step  $\Delta t = 0.1$ . The initial condition for the mRNA concentrations is taken as  $\mathbf{x}_0 = 1001$ , unless stated differently.

### 4.3. Interacting Networks: The Interconnection

What would happen to the whole system if you would add a connection between the two networks? The influence of an interconnection depends on several factors. In the following subsections we shall investigate the influence of the weight of the interconnection, the placement of the interconnection and the amount of interconnections.

#### 4.3.1. Interconnection of Weight One

First we start with an interconnection of weight one. The interconnection changes our matrix

$A = \begin{bmatrix} A_1 & 0 \\ 0 & A_2 \end{bmatrix}$  slightly. Instead of a block diagonal structured matrix, we have to add an off-diagonal

block (B) in the following way:  $A = \begin{bmatrix} A_1 & B \\ B^T & A_2 \end{bmatrix}$ . Here B is the “interconnection” matrix. It represents the undirected edge between node  $i (\in \{0, 1, 2, 3\})$  in network 1 and node  $j (\in \{4, 5, 6, 7\})$  in network 2. The matrix B represents a directed edge from node  $j$  to node  $i$ , while the matrix  $B^T$ , the transpose of B, represents a directed edge from node  $i$  to node  $j$ . For now we assume that it is a bidirectional

connection with equal weight  $\epsilon$ .

For this example we will take  $\epsilon = 1$  and we put a bidirectional edge between node 3 and node 4. So, the edges (3,4) and (4,3) are added. The matrix B then takes the form:

$$B = \begin{bmatrix} 0 & 0 & 0 & 0 \\ 0 & 0 & 0 & 0 \\ 0 & 0 & 0 & 0 \\ \epsilon & 0 & 0 & 0 \end{bmatrix} \quad B^T = \begin{bmatrix} 0 & 0 & 0 & \epsilon \\ 0 & 0 & 0 & 0 \\ 0 & 0 & 0 & 0 \\ 0 & 0 & 0 & 0 \end{bmatrix}$$

This interconnection of weight  $\epsilon = 1$  is visualised in Figure 4.5. Since  $A_1$  and  $A_2$  are fully connected matrices, the directions and corresponding weights are dropped. Otherwise the figure would become too messy.

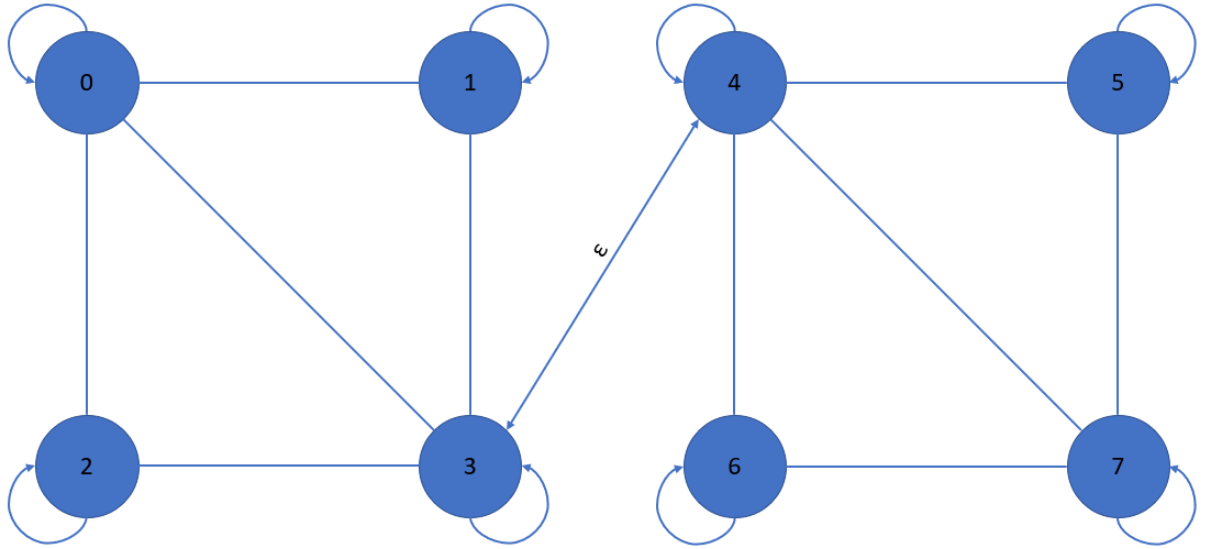


Figure 4.5: Graphical representation of an interacting network. Network 1 consists of the nodes  $X_i$ , with  $i \in \{0, 1, 2, 3\}$ . Network 2 consists of the nodes  $X_j$ , with  $j \in \{4, 5, 6, 7\}$ . The nodes 3 and 4 are interacting. This is represented by an interconnection, or an edge, between nodes 3 and 4. This edge has weight  $\epsilon = 1$ .

Next, the eigenvalues of the system with interconnection  $\epsilon = 1$  are checked. In Figure 4.6 the eigenvalues are plotted. Rounding them off gives us the following eigenvalues:

$$\lambda_{0,1} = -1.08 \pm 0.61i \quad \lambda_{2,3} = 0.31 \pm 0.39i \quad \lambda_{4,5} = -0.40 \pm 0.47i \quad \lambda_6 = -0.34 \quad \lambda_7 = -0.50$$

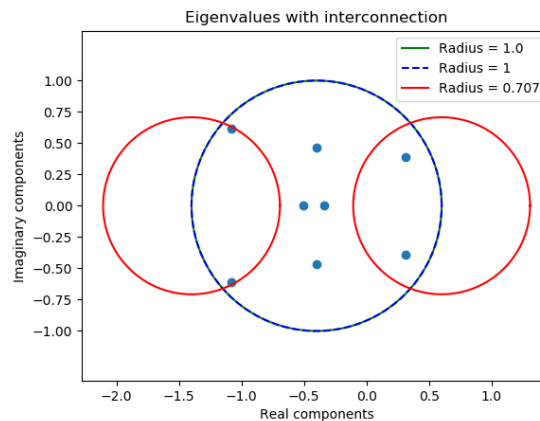


Figure 4.6: Eigenvalue distribution of two interconnected networks with interconnection weight  $\epsilon = 1$ . The red circles give a bound on the distribution of the outlier eigenvalue caused by the interconnection. The center of this circle is  $(-W \pm \epsilon, 0)$ , the radius of this circle is  $\frac{1}{n^4}$

You might have noticed that there are also two red circles visible in Figure 4.6. The circles have (a rather arbitrary) radius  $\frac{1}{n^{\frac{1}{4}}}$  (Tao, 2013) and center  $(-W \pm \epsilon, 0)$ . Where  $n$  is presumably the amount of nodes of the network with the highest average connectivity  $\langle k \rangle$ . These circles give another bound on the eigenvalues caused by the weight of the interconnection  $\epsilon$ . An outlier, with respect to Girko's circle, could have a huge effect on the stability and development of the system, which becomes more clear in subsection 4.3.3.

The fact that such an outlier exists around  $\epsilon$  can be proven for very small systems, think of a 4x4 system where each network consists of 2 nodes, by computing the characteristic polynomial. With this characteristic polynomial a simple assumption is required that  $\epsilon \gg A_{ij}$  to obtain a characteristic polynomial of the form  $P(\lambda) \approx (\lambda - \epsilon - W)(\lambda + \epsilon - W)F(\lambda)$ . Where  $F(\lambda)$  is some leftover polynomial for the other 2 eigenvalues. The existence of an outlier also seems to hold numerically for larger systems, however a proof using the characteristic polynomial is impossible for 'larger' matrices.

Maybe the reader could think of some proof using perturbation theory or spectral theory, but this did not work out for me. To make it even more vague, the magnitude and the amount of outliers also depend on the amount of interconnections and the placement of the interconnections, which is treated shortly in subsection 4.3.5. With this in mind the proof should also take the placement and the number of interconnections into account, whether this exists remains a question.

Resuming our story; since some eigenvalues have a positive real part, the solution is unstable. This coincides with the numerical solution in Figure 4.7. The solution keeps oscillating from negative concentrations to positive concentrations, and increases in amplitude. An inhibitory effect together with a large negative deviation with respect to the equilibrium can cause a huge increase in concentration. This is clearly a flaw from the current model. The eigenvalue distribution of the linear model is however important to understand the non-linear model later on in Chapter 5.

Besides the eigenvalues, the eigenvectors have also changed. Before the eigenvectors only had at most 4 non-zero entries. Now the eigenvectors belonging to the eigenvalues with a positive real part have 8 non-zero entries:

$$v_3 = \begin{bmatrix} -0.06 + 0.04i \\ -0.08 + 0.06i \\ -0.04 + 0.03i \\ 0.50 - 0.09i \\ 0.57 \\ 0.252i \\ -0.07 + 0.35i \\ 0.27 + 0.37i \end{bmatrix} \quad v_4 = \begin{bmatrix} -0.06 - 0.04i \\ -0.08 - 0.06i \\ -0.04 - 0.03i \\ 0.50 + 0.09i \\ 0.57 \\ -0.252i \\ -0.07 - 0.35i \\ 0.27 - 0.37i \end{bmatrix} = \text{conjugate}(v_3)$$

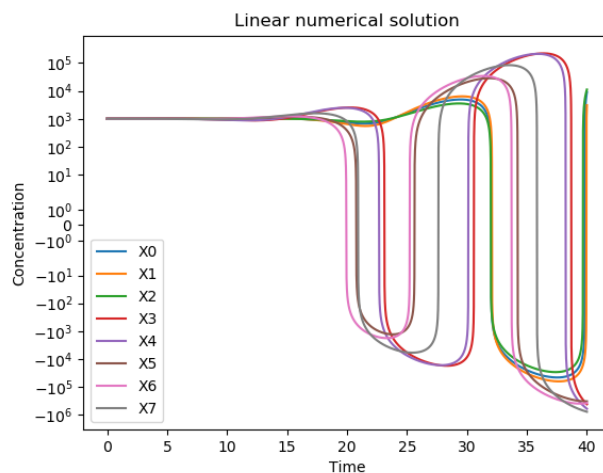


Figure 4.7: Numerical solution for the linear model of two interconnected networks, where the interconnection weight is  $\epsilon = 1$ . The solution shows oscillating, but divergent behaviour.

### 4.3.2. Small Interconnection

In the following example we take  $\epsilon = 0.1$ . An interconnection has a ‘small’ weight if its magnitude is smaller than most entries  $A_{ij}$  in absolute value. This is a rather short subsection, since a small weighted interconnection does not influence the behaviour of the system at all. There is only a very slight difference in the numerical solution, which might be visible if you compare Figure 4.9 and the previous Figure 4.7 closely. The stability however remains the same. This is simply due to the fact that a small weighted interconnection is too small to have an influence on the system, since the other interaction rates are a lot larger.

For completeness the eigenvalue distribution is still given in Figure 4.8, by inspection this looks the same as the eigenvalue distribution of the system without interconnection. This also explains the similar behaviour of the solution, as all real parts are still negative. In the next subsection we will explore a large weighted interconnection.

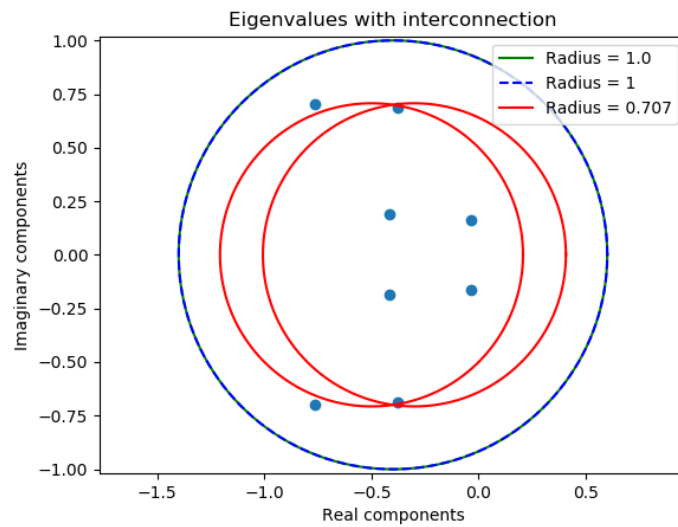


Figure 4.8: Eigenvalue distribution of two interconnected networks with interconnection weight  $\epsilon = 0.1$ . The explanation of the red circles is the same as above.

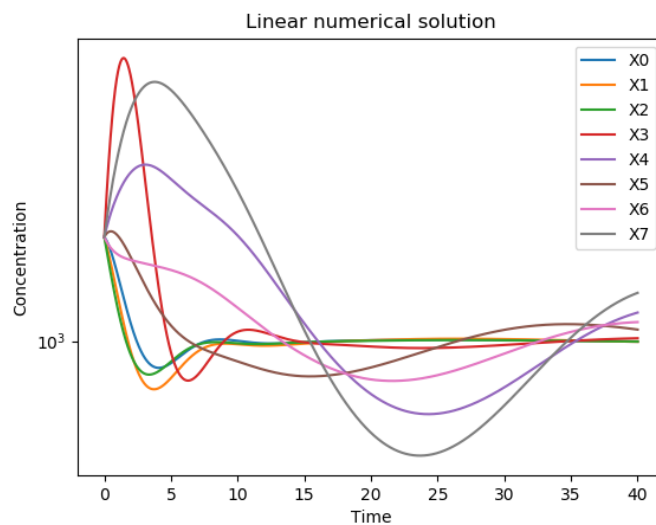


Figure 4.9: Numerical solution for the linear model of two interconnected networks, where the interconnection weight is  $\epsilon = 0.1$ . The numerical solution is similar to the numerical solution without interconnection.

### 4.3.3. Large Interconnection

In this subsection we will study an interconnection with a ‘large’ weight. An interconnection has a large weight if its magnitude is (far) beyond the expected radius of Girko’s circle. As reminder, the radius of Girko’s circle was  $\rho = \sigma_A \sqrt{\langle k \rangle}$ . If we then take the weight  $\epsilon$  about 3 times as big, then the assumptions of the characteristic ‘proof’ from subsection 4.3.1 hold.

In this case we will take  $\epsilon = 3$ , where Girko’s circle has radius 1. It is then expected that there are 2 ‘outlier’ eigenvalues around  $(-W \pm \epsilon, 0)$  with radius  $\frac{1}{n^4}$ . These are the red circles in the eigenvalue plot Figure 4.10.

From this figure it is visible that there are 2 eigenvalues with a positive real part. These eigenvalues and their corresponding eigenvector, rounded off to 2 decimals, are:

$$\lambda_1 = 0.35 \quad \text{and} \quad \lambda_2 = 2.43$$

$$v_1 = \begin{bmatrix} 0.03 \\ 0.04 \\ 0.02 \\ -0.19 \\ -0.08 \\ 0.32 \\ 0.57 \\ 0.73 \end{bmatrix} \quad \text{and} \quad v_2 = \begin{bmatrix} -0.03 \\ -0.04 \\ -0.02 \\ 0.7 \\ 0.69 \\ -0.02 \\ -0.13 \\ 0.01 \end{bmatrix}$$

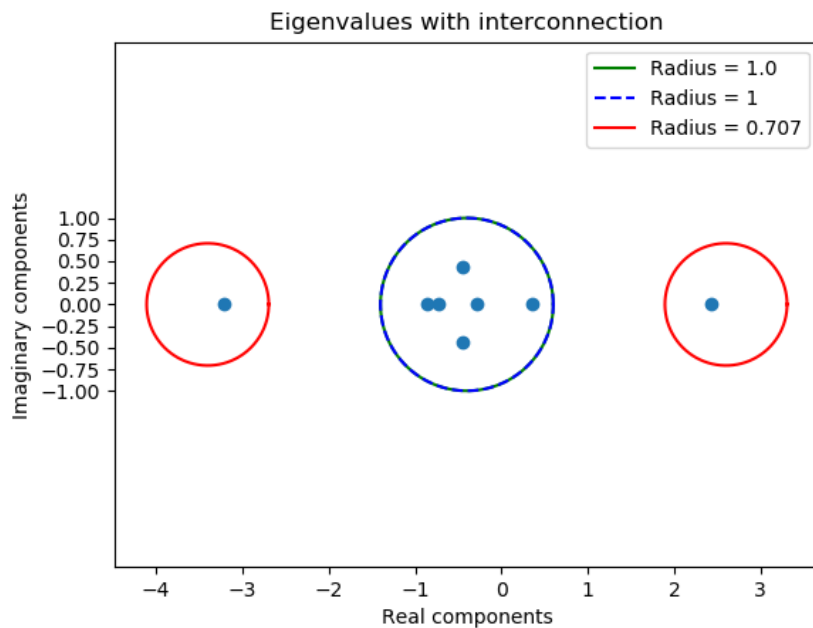


Figure 4.10: Eigenvalue distribution of two interconnected networks with interconnection weight  $\epsilon = 3$ . Due to the large interconnection weight 2 huge outliers arise.

If we take a look at the numerical solution Figure 4.11, the beginning is quite stable. However, Around  $t = 3$ , there is a sudden change in the solution.

Using the eigenvalues and eigenvectors this can be explained. The solution is of the form as described by equation 4.3. This equation is dominated by the eigenvalues with a positive real part. At the beginning  $\exp(\lambda_1)v_1$  cancels out  $\exp(\lambda_2)v_2$ . The small possible fluctuations are not visible on this scale.

Sooner rather than later  $\exp(\lambda_2)$  outgrows  $\exp(\lambda_1)$ , that is  $\exp(\lambda_2) \gg \exp(\lambda_1)$ . This seems to happen around  $t = 3$  already, after which the solution grows in the direction of  $v_2$ . Indeed the concentrations  $X_3, X_4$  and  $X_7$  diverge to  $+\infty$ , while the rest diverges to  $-\infty$ . This corresponds with the sign of

the entries of  $v_2$ . Note that the red line of  $X_3$  and the purple line of  $X_4$  coincide in the figure, due to the scaling.

This is a great example to show that an interconnection of large weight can have a huge influence on the stability of the solution. Without the interconnection, the system was asymptotically stable. Now, the system shows gigantic divergent behaviour.

It also shows that the eigenvalue with the biggest positive real part dominates the solution. This eigenvalue is also known as the maximum Lyapunov exponent (MLE), which was introduced in subsection 3.2.

In the following subsection we will explore the directed interconnection.

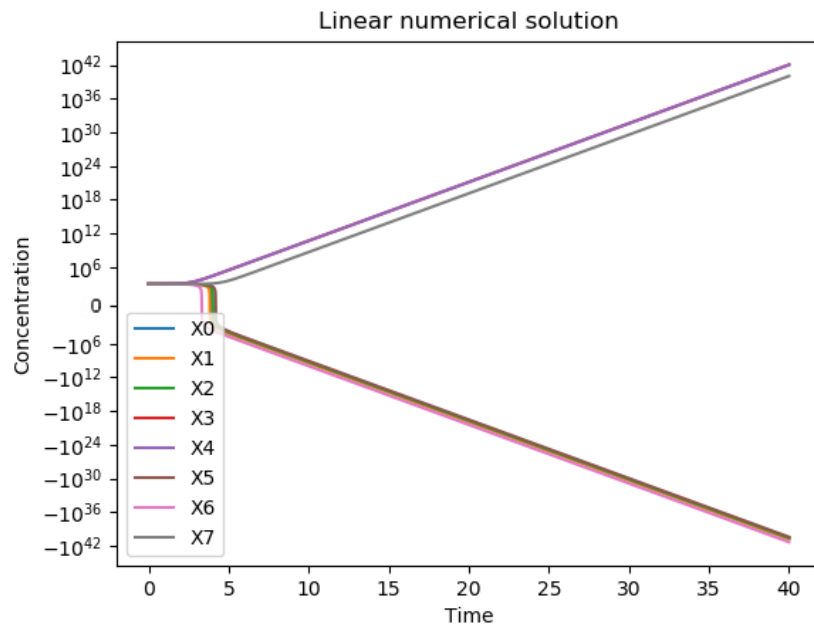


Figure 4.11: Numerical solution for the linear model of two interconnected networks, where the interconnection weight is  $\epsilon = 3$ . The solution shows enormous divergent behaviour.

#### 4.3.4. Directed Interconnection

In this subsection we will consider the directed interconnection. Where a directed interconnection is defined as an interconnection that is one-sided. Graphically the double-sided arrow from Figure 4.5 with weight  $\epsilon$  turns into a one-sided arrow.

In this example the arrow can either point from node 4 to node 3 (4,3) or from node 3 to node 4 (3,4). In the first case we get the interaction matrix of the form  $\begin{bmatrix} A_1 & B \\ 0 & A_2 \end{bmatrix}$ . So network 1 is influenced. In the second case we obtain the interaction matrix  $\begin{bmatrix} A_1 & 0 \\ B^T & A_2 \end{bmatrix}$ . So network 2 is influenced. Where  $A_1, A_2, B, B^T$  are defined as in subsection 4.3.1.

To make the figures more interesting and to make the influence of a directed interconnection more clear,  $\epsilon$  has the large weight 3. The numerical results of the first case are plotted in Figure 4.12b, together with the (scaled) numerical solution Figure 4.12a of subsection 4.2. In this way the influence of a directed interconnection can easily be compared to the system without interconnections. The figure is scaled such that the numbering of the  $y$ - and  $x$ -axes are equal.

We see that the numerical solution of the concentrations  $X_4$  up to  $X_7$  remain the same, they do not get influenced in any way by the directed interconnection. The course of the concentrations of  $X_0$  up to  $X_3$  however, do differ. As expected, only the system which the arrow points towards is influenced.

The numerical results of the second case are plotted in Figure 4.13b, together with the (scaled) numerical solution Figure 4.13a. In this case network 2 gets influenced by network 1, so only the course of the concentrations of  $X_4$  up to  $X_7$  will differ.

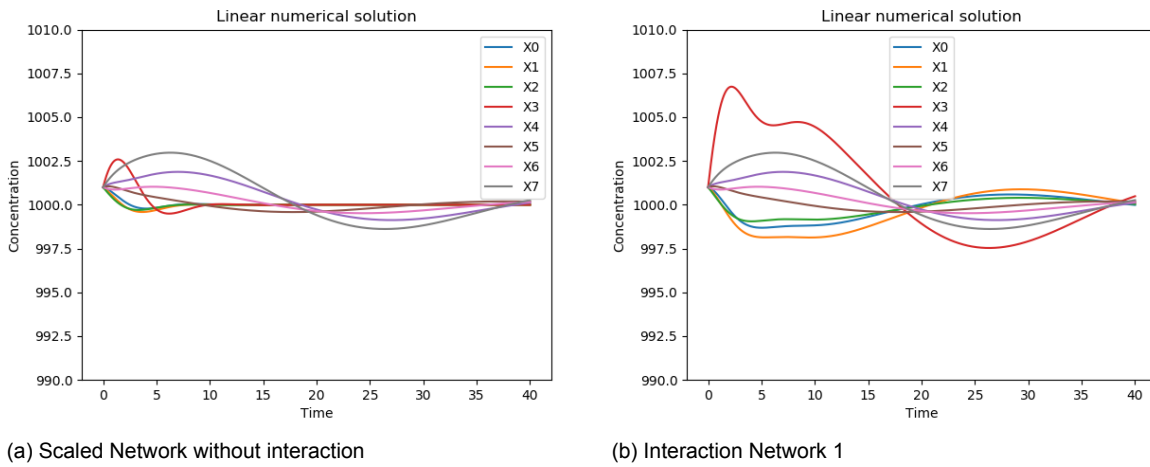


Figure 4.12: (a) Linear numerical solution of the system without any interconnections. It is the scaled version of Figure 4.4 to fit the scaling of graph (b). (b) Linear numerical solution of the network with a directed interconnection from node 4 to node 3. Only network 1 is influenced.

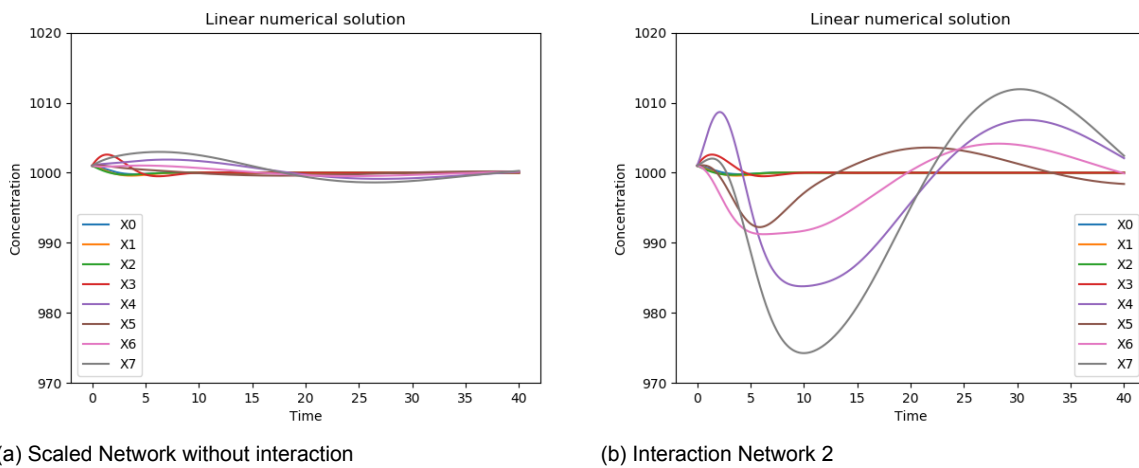


Figure 4.13: (a) Linear numerical solution of the system without any interconnections. It is the scaled version of Figure 4.4 to fit the scaling of graph (b). (b) Linear numerical solution of the network with a directed interconnection from node 3 to node 4. Only network 2 is influenced.

These conclusions follow the theory of Linear Algebra. In the Linear Algebra it is known that the eigenvalues of a block triangular matrix of the form

$$M = \begin{bmatrix} A & B \\ 0 & C \end{bmatrix} \quad \text{or} \quad M = \begin{bmatrix} A & 0 \\ B & C \end{bmatrix}$$

do not depend on the block B at all. Because the characteristic polynomial is given by  $P_\lambda(M) = P_\lambda(A)P_\lambda(C)$ . So, the eigenvalues of a directed interaction matrix are equal to the eigenvalues of an interaction matrix without interconnections.

An important consequence is then that the stability of the solution remains the same. If the solution was asymptotically stable, then the solution remains asymptotically stable. Although, the eigenvectors do change.

For  $M = \begin{bmatrix} A & B \\ 0 & C \end{bmatrix}$ : if  $\mathbf{b}_i$  is an eigenvector of A with eigenvalue  $\lambda_i$ , then  $\begin{bmatrix} \mathbf{b}_i \\ 0 \end{bmatrix}$  is an eigenvector of M

with eigenvalue  $\lambda_i$ . But, if  $\mathbf{d}_j$  is an eigenvector of  $C$  with eigenvalue  $\lambda_j$ , then  $\begin{bmatrix} 0 \\ \mathbf{d}_j \end{bmatrix}$  is not necessarily an eigenvector of  $M$ . The eigenvector of  $M$  with eigenvalue  $\lambda_j$  is instead of the form  $\begin{bmatrix} \mathbf{h}_j \\ \mathbf{d}_j \end{bmatrix}$ , where  $\mathbf{h}_j$  and  $\mathbf{d}_j$  satisfy  $(\lambda_j \mathbf{I} - A)\mathbf{h}_j = B\mathbf{d}_j$  (Sadun, 2008).

This tells us that the eigenvalues of  $C$  influence network 1, with eigenvector  $\mathbf{h}_j$ . So, if the stability of network 2 differs from the stability of network 1, the stability of the solution of network 1 can actually change. This will only happen if the stability of network 2 is more 'dominant' than the stability of network 1. In the sense that divergent is more dominant than oscillatory and convergent behaviour, and that oscillatory behaviour is more dominant than convergent behaviour.

The case where  $M$  takes the other form is analog. In the next subsection we will treat the last type of interconnections shortly: the number and placement of interconnections.

### 4.3.5. The Number and Placement of Interconnections

In this subsection we will explore the influence of the number of bidirectional interconnections and the placement of interconnections. Let us first define these terms.

The number of interconnections is simply the amount of bidirectional edges connecting a node from network 1 to network 2. For our system we can create at most 16 bidirectional interconnections, as each node (0 up to 3) can have at most 4 outgoing edges to the nodes from network 2 (4 up to 7).

The placement of an interconnection has to do with which nodes are connected to which. If you have a total of 4 interconnections, we can for example have the edges (0, 4), (0, 5), (0, 6) and (0, 7) or the edges (0, 4), (1, 5), (2, 6), (3, 7). This results in two different interaction matrices. Many more combinations are possible with 4 interconnections.

The number and placement of interconnections can not be checked separately, as they are connected in some way. In the sense that the distribution of the eigenvalues are determined by the number of interconnections and the placement of the interconnections at the same time. It is also impossible to show a figure of each case, as for every number of interconnections there are a lot of different placements possible.

Therefore, let us start with a histogram (Figure 4.14) of the distribution of the real parts for different amounts of interconnections and different placements of interconnections, which are generated randomly. 1000 random matrices were generated in this way for this histogram.

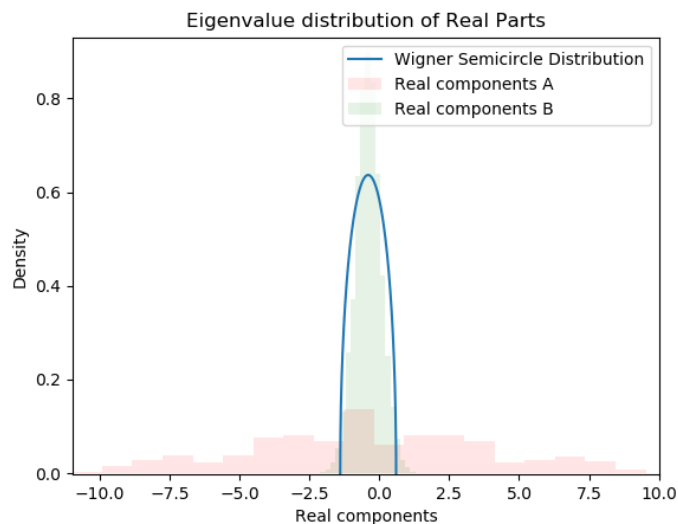


Figure 4.14: Histogram of the real parts of the eigenvalues for 1000 randomly interconnected networks. The size of the matrix is  $8 \times 8$ , which consists of 2 networks, each of 4 nodes. The interaction matrices were generated with diagonal elements  $W = 0.4$ , edge probability  $p = 1$  and  $\epsilon = 3$ . The entries of the interaction matrix are taken from a  $N(0, \frac{1}{4})$  distribution.

Here A is a randomly generated interaction matrix, which consists of two networks, each of 4 nodes.

The interaction rates are taken from a normal distribution with mean 0 and variance  $\frac{1}{4}$ . The amount of interconnections and the placement of the interconnections are generated randomly. The weight of the interconnections is  $\epsilon = 3$ . B is the same interaction matrix as A, but without any interconnections. That is

$$A = \begin{bmatrix} A_1 & \text{Interconnections} \\ \text{Interconnections}^T & A_2 \end{bmatrix} \quad \text{and} \quad B = \begin{bmatrix} A_1 & 0 \\ 0 & A_2 \end{bmatrix}$$

Since the sizes of the matrices are only  $8 \times 8$ , the eigenvalue distribution of matrix B does not converge to Wigner's semicircle perfectly. It would for larger matrices. In the histogram it is visible that the eigenvalues of matrix A, with randomly placed interconnections of weight  $\epsilon = 3$  are distributed over approximately the range  $(-10, 10)$ . There is not any visible pattern.

What would happen if we take the number of interconnections constant, say 4, and place them randomly? In that case we obtain the following histogram:

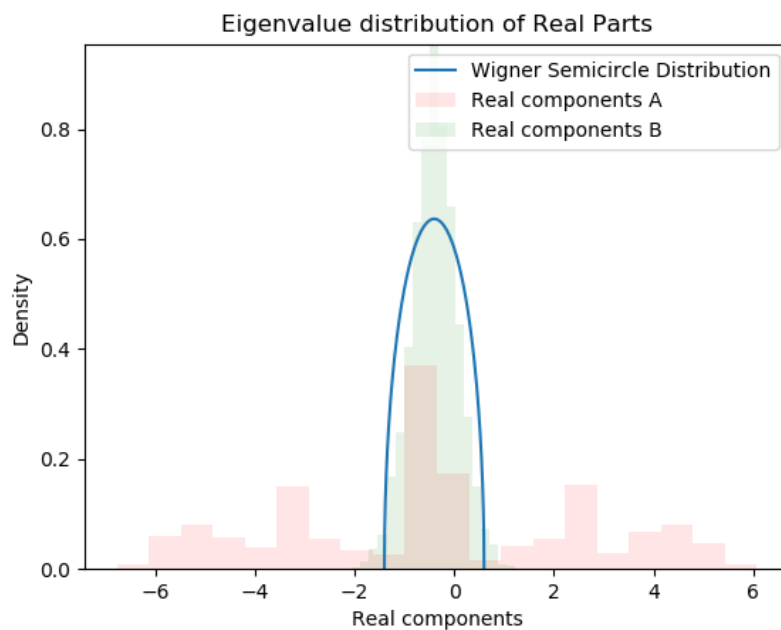


Figure 4.15: Histogram of the real parts of the eigenvalues for 1000 networks with 4 interconnections placed randomly. The size of the matrix is  $8 \times 8$ , which consists of 2 networks, each of 4 nodes. The interaction matrices were generated with diagonal elements  $W = 0.4$ , edge probability  $p = 1$  and  $\epsilon = 3$ . The entries of the interaction matrix are taken from a  $N(0, \frac{1}{4})$  distribution.

There is still no visible pattern, so how do these randomly placed interconnections influence the eigenvalue distribution? There is much unknown, but we have found the following numerical result: If 4 interconnections are placed in a distinct row and column, then we obtain 8 outliers distributed on the same red circles from before. In general if we have  $n$  interconnections placed in distinct rows and columns, then we obtain  $2n$  outliers.

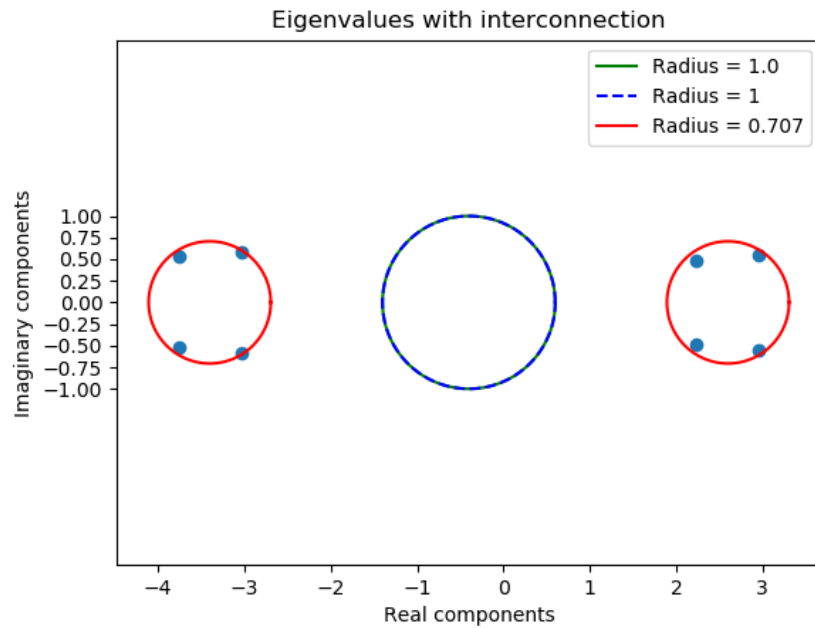


Figure 4.16: Eigenvalue distribution of a network with 4 bidirectional interconnections placed in distinct rows and columns. 8 outliers arise distributed on the red circles.

If the 4 interconnections are not placed in four distinct rows and columns, then the eigenvalues are distributed differently again. In the following Figure the 4 interconnections are placed in only 3 distinct rows and columns. This time we have 6 outliers, not necessarily distributed on the red circles.

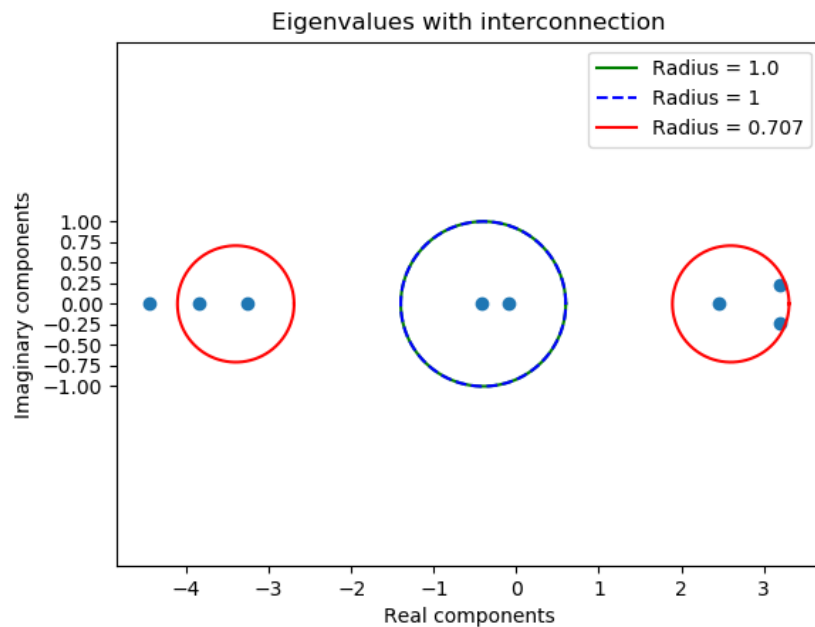


Figure 4.17: Eigenvalue distribution of a network with 4 bidirectional interconnections placed in only 3 distinct rows and columns. 6 outliers arise, not necessarily distributed on the red circles.

The feeling is that the amount of distinct rows and columns give the amount of outliers (times 2). This is hard to show in general, since there are way too many cases to consider.

We end this subsection with the eigenvalue distribution of a fully interconnected matrix, that is a matrix with 16 interconnections of weight 1:

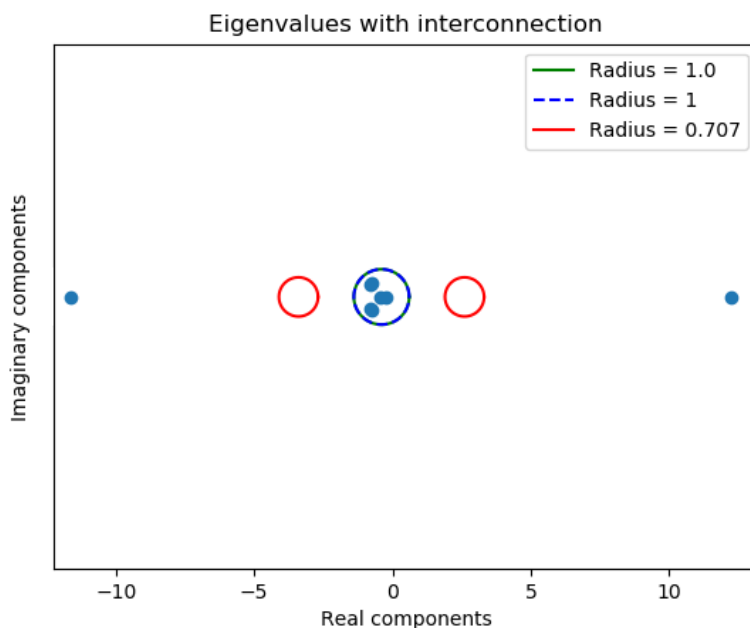


Figure 4.18: Eigenvalue distribution of a network with 16 bidirectional interconnections. A huge outlier arises, far beyond the red circle.

In this case there is only one huge outlier. As you can see the influence of the number of interconnections and the placement of these interconnections remains puzzling. It is unknown how this works. It is hard to reason with this due to the amount of cases, and due to the fact that an idea should bring the placement and the number of interconnections together.

In the past 5 subsections we have seen several possibilities of placing an interconnection. There are of course many more possibilities. Think of placing several directed edges, or think of different weighted interconnections. However, in general it is unknown for us whether it is possible to predict the new eigenvalues and eigenvectors by using the knowledge from the original matrix  $A$  without interconnection. The question how exactly interconnections influence the eigenvalues of a matrix remains open.

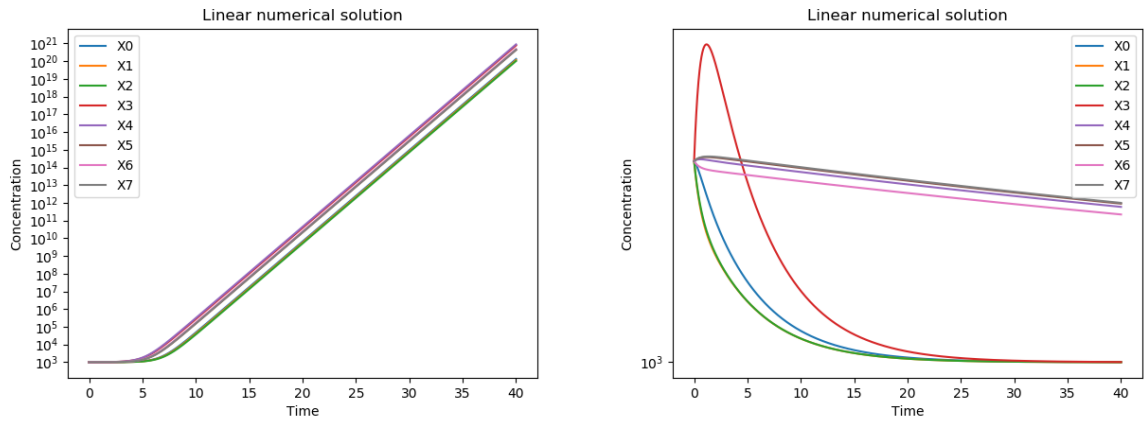
In the upcoming two subsections we will complete the study of the linear model by checking some special interaction matrices. First, we will study a strictly positive interaction matrix, then we will inspect a strictly negative interaction matrix.

#### 4.4. Strictly Positive Interaction Matrix

In this case it is checked what happens when a strictly positive interaction matrix is created. Although, the diagonal remains the same with entries  $-0.4$  to ensure that Girko's circle does not shift along. That is, the entries  $A_{ij}$  become  $|A_{ij}|$  for  $i \neq j$ . Including a bidirectional interconnection of weight one between node 3 and 4 gives us the same interaction matrix as in subsection 4.3.1, but with positive entries  $A_{ij}$ .

Having a strictly positive interaction matrix means that every mRNA concentration has an excitatory effect on another mRNA concentration. The inhibitory effect of the mRNA concentration on itself remains intact, due to the choice of the diagonal. Since almost all entries of this interaction matrix are positive we expect that the mRNA concentrations keeps increasing. This is visible in Figure 4.19a.

Of course it remains possible to have a stable solution if the diagonal is chosen negative enough, such that there is no eigenvalue with a positive real part. In that case the inhibitory effect of the diagonal entries eventually exceeds the total excitatory effect of the off-diagonal entries. Choosing for example  $W = 1.3$ , does the trick, rather slow, in this case (Figure 4.19b)



(a) Linear numerical solution for a strictly positive interaction matrix

(b) Linear numerical solution for a strictly positive interaction matrix with diagonal elements  $W=1.3$

Figure 4.19: (a) Linear numerical solution with diagonal elements  $W = 0.4$ . The solution diverges to  $+\infty$ . (b) Linear numerical solution with diagonal elements  $W = 1.3$ . The solution converges to its equilibrium  $\mathbf{x}^0$ .

It should be noted that the solution highly depends on the initial concentrations of the mRNA. In the above case the initial concentration is  $\mathbf{x}_0 = 1001$  for each mRNA. If we change this to  $\mathbf{x}_0 = 999$  the solution diverges to  $-\infty$  (Figure 4.20). This is due to the fact that our linear model (equation 4.1) is written as  $\dot{\mathbf{x}} = A(\mathbf{x} - \mathbf{x}^0)$ . So, if we start beneath  $\mathbf{x}^0$ , then  $\mathbf{x} - \mathbf{x}^0 < 0$  from the start. Which results in a 'strictly' positive matrix times a strictly negative column vector. Hence,  $\dot{\mathbf{x}} < 0$ .

This is not a flaw of the model. In the equilibrium the natural excitatory and inhibitory effects of the model cancels each other, the effects are in balance. If you start beneath the equilibrium, then the mRNA concentrations can not overcome the standard inhibitory effects.

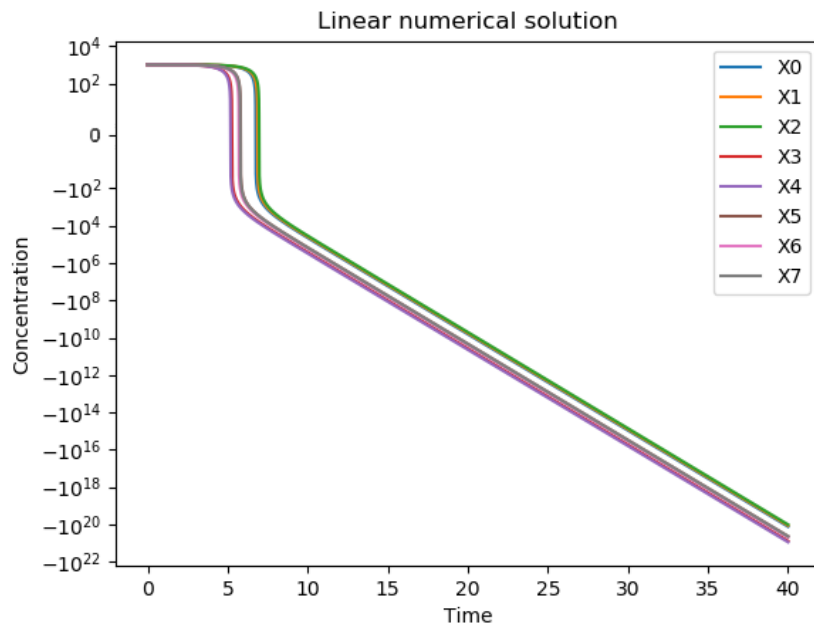


Figure 4.20: Linear numerical solution with diagonal elements  $W = 0.4$ . The initial condition  $\mathbf{x}_0 = 999$  is taken, instead of  $\mathbf{x}_0 = 1001$ . This results in a diverging solution to  $-\infty$ .

## 4.5. Strictly Negative Interaction Matrix

In this subsection we consider a strictly negative interaction matrix. This means that every concentration has an inhibitory effect on the other concentrations and on itself. At first thought it is expected that all concentrations become negative or that all concentrations go to zero. However, in the current model an inhibitory effect multiplied with a negative concentration causes a huge excitatory effect. Which could cause an increase in some RNA concentrations. This is clearly a flaw in the current model.

Since we are speaking of concentrations, we should add the restriction  $\mathbf{x} \geq 0$  to the model. Concentrations are after all non-negative. This restriction makes the model non-linear. In the next chapter this non-linear model will be studied.

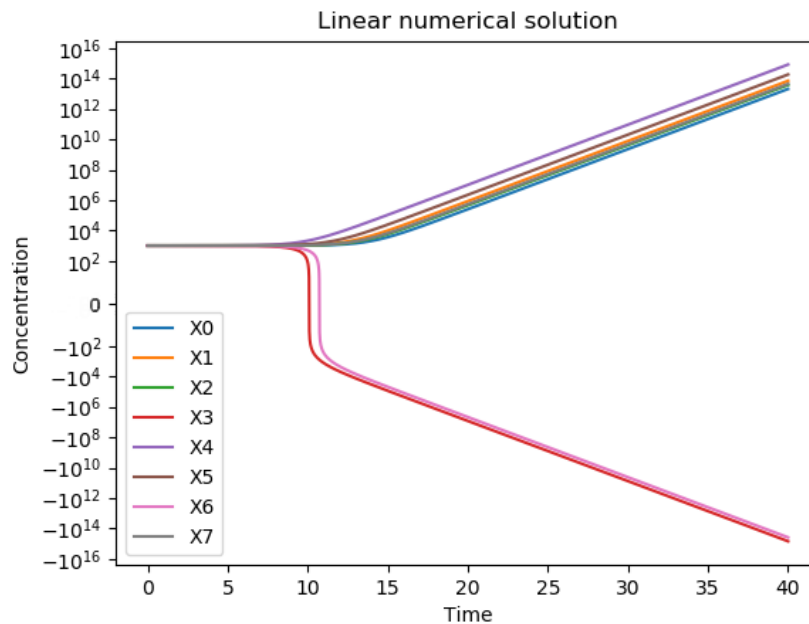


Figure 4.21: Linear numerical solution for a strictly negative interaction matrix with diagonal elements  $w = 0.4$ . Some concentrations diverge to  $+\infty$ , others to  $-\infty$ . A large negative concentration with an inhibitory effect can cause a huge excitatory effect.



# 5

## Nonlinear Model for Gene Networks

In this chapter the non-linear model from equation 2.1 is discussed, which is repeated for convenience.

$$\begin{aligned}\dot{\mathbf{x}} &= A(\mathbf{x} - \mathbf{x}^0) \\ \mathbf{x} &\geq 0\end{aligned}\tag{5.1}$$

The non-linear model uses the same system of linear differential equations as the linear model, but with one extra constraint: concentrations are non-negative. Physically it is simply not possible to have a negative concentration and this should therefore be added to the model.

We will explore this non-linear model by first comparing some numerical solutions of the non-linear model with the linear model of Chapter 4 (Section 5.1). Then, we will check some general properties of the nonlinear model: the on and off distribution of nodes in Section 5.2. Where a node is on if its concentration is larger than zero, and a node is off if its concentration is zero. This leads to a varying average connectivity  $\langle k \rangle$  over time, where the maximum Lyapunov exponent (MLE) finally comes into play in Section 5.3.

### 5.1. Numerical Solutions of the Nonlinear Model

In this section we will compare some interesting figures of the numerical solutions of the linear model with the numerical solutions of the non-linear model. Interesting figures of Chapter 4 are figures where the concentration of certain nodes become negative. After all, if no concentration becomes negative then the non-negative restriction could be omitted. Without this restriction we simply obtain the linear model again, and then the solution is of course the same as the linear model.

Let us first repeat our interaction matrix  $A$ , which was used in Chapter 4. This matrix modelled the interaction between 2 networks of 4 nodes.  $A$  was a block diagonal matrix of the form  $A = \begin{bmatrix} A_1 & 0 \\ 0 & A_2 \end{bmatrix}$ .

Where  $A_1$  and  $A_2$  were given by

$$A_1 = \begin{bmatrix} -W & -0.38 & 0.74 & -0.12 \\ -0.22 & -W & 0.34 & -0.16 \\ -0.44 & 0.21 & -W & -0.10 \\ 1.93 & 0.60 & 0.22 & -W \end{bmatrix}$$
$$A_2 = \begin{bmatrix} -W & -0.16 & 1.10 & -0.08 \\ 0.11 & -W & 0.89 & -0.36 \\ -0.54 & 0.24 & -W & 0.43 \\ 0.18 & 0.44 & 0.74 & -W \end{bmatrix}$$

The diagonal weights  $W$  were chosen as  $W = 0.4$ .

Now that we have defined our system, we will calculate and compare the non-linear solutions with the following 4 linear solutions from Figures 4.7, 4.11, 4.20 and 4.21. The case of an interaction matrix with weight one, the case of an interaction matrix with large weight, the case of a strictly positive interaction matrix, and the case of a strictly negative interaction matrix, respectively. These figures will be treated and repeated in the same order in the following four subsections separately.

### 5.1.1. Interconnection of Weight One

First on the list is the system where an interconnection of weight one was added, Figure 4.7. This changed our interaction matrix  $A$  to  $A = \begin{bmatrix} A_1 & B \\ B^T & A_2 \end{bmatrix}$ . With  $B$  and  $B^T$  given by

$$B = \begin{bmatrix} 0 & 0 & 0 & 0 \\ 0 & 0 & 0 & 0 \\ 0 & 0 & 0 & 0 \\ 1 & 0 & 0 & 0 \end{bmatrix} \quad B^T = \begin{bmatrix} 0 & 0 & 0 & 1 \\ 0 & 0 & 0 & 0 \\ 0 & 0 & 0 & 0 \\ 0 & 0 & 0 & 0 \end{bmatrix}$$

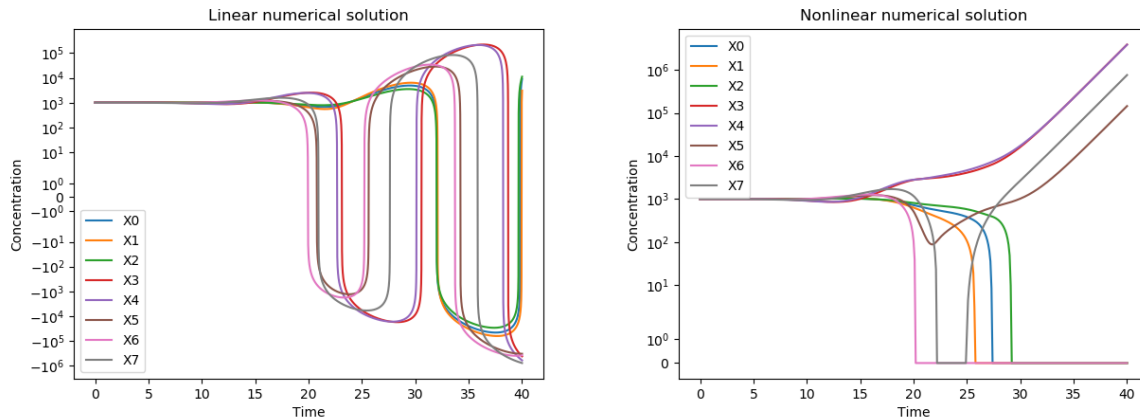
Below the numerical solution is plotted for the linear model (Figure 5.1a) and the nonlinear model (Figure 5.1b). Clearly the solutions differ a lot. In the linear case there was some oscillatory behaviour combined with divergent behaviour. In the nonlinear case it eventually ends with some concentrations showing divergent behaviour. The comparison is to show that the solutions are different.

Let us zoom in on the nonlinear solution. First note that the non-negative restriction is working. Some nodes go to zero and stay zero, these nodes are considered off.

However, it is possible for a node to go on again: for example the gray node  $X_7$  goes to zero, remains zero for some time and then becomes positive again. This is due to the interaction rates. There is a moment where the inhibitory effects are bigger than the excitatory effects such that the concentration goes to zero, but eventually the excitatory effects end up bigger than the inhibitory effects and then it keeps growing.

Secondly we notice that there is some kind of stable behaviour in the time window  $t = 0$  up to  $t = 30$ . Where the time window  $t = 0$  up to  $t = 20$  is still part of the linear model. After  $t = 30$  the solution diverges.

It turns out that this change of behaviour is not a coincidence. For larger networks this can be explained by reasoning with the average connectivity ( $k$ ) and the radius of Girko's circle. But for smaller networks this does not work, since they do not converge to Girko's distribution.



(a) Linear numerical solution

(b) Nonlinear numerical solution

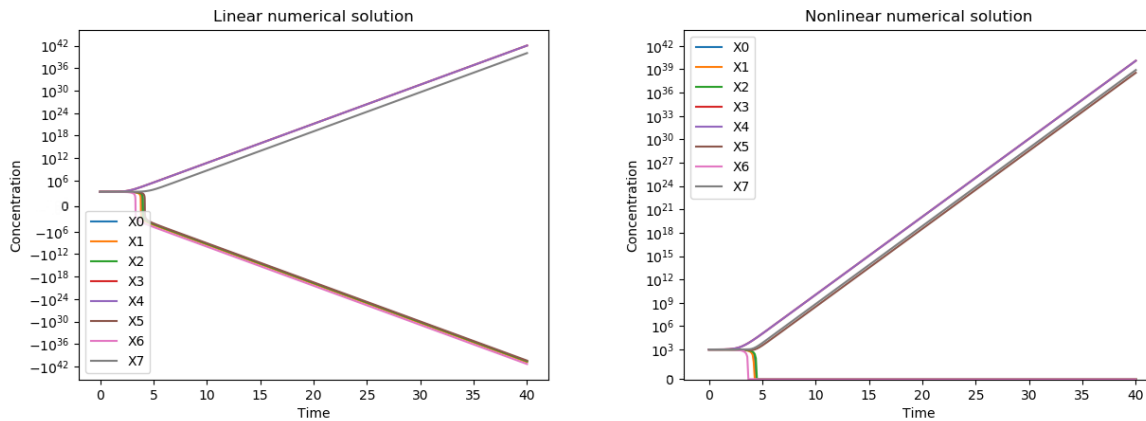
Figure 5.1: (a) Numerical solution for the linear model of two interconnected networks, where the interconnection weight is  $\epsilon = 1$ . The solution shows oscillating, but divergent behaviour. (b) Numerical solution for the nonlinear model of two interconnected networks, where the interconnection weight is  $\epsilon = 1$ . The solution shows partly stable behaviour in the time window  $t \in [0, 30]$  and shows divergent behaviour for  $t > 30$ . Some nodes become zero and stay zero, one node becomes active again.

### 5.1.2. Large Interconnection

Second on the list is the system where an interconnection of weight three was added, Figure 4.11. This interconnection caused a large eigenvalue with real part 3.

In figure 5.2a the linear solution is plotted and in Figure 5.2b the nonlinear solution. The non-negative restriction does not seem to have a lot of influence in this case, apart from keeping some concentrations at zero. This is probably due to the fact that the eigenvalue with real part 3 determines the course of the solution. There is one 'big' difference, the concentration of node 5 diverges to  $+\infty$ ,

instead of  $-\infty$ . It seems like the interaction with node 4, with interaction rate 0.11, takes the upper hand and causes node 5 to diverge to  $+\infty$  as well.



(a) Linear numerical solution

(b) Nonlinear numerical solution

Figure 5.2: (a) Numerical solution for the linear model of two interconnected networks, where the interconnection weight is  $\epsilon = 3$ . The solution shows enormous divergent behaviour. (b) Numerical solution for the nonlinear model of two interconnected networks, where the interconnection weight is  $\epsilon = 3$ . The solution of some concentrations shows enormous divergent behaviour, while others converge to 0 and stay at zero.

### 5.1.3. Strictly Positive Interaction Matrix

Third on the list is the system with a strictly positive interaction matrix, apart from the diagonal (Figure 4.20). It also included an interconnection of weight one, in the same place as before. So, here

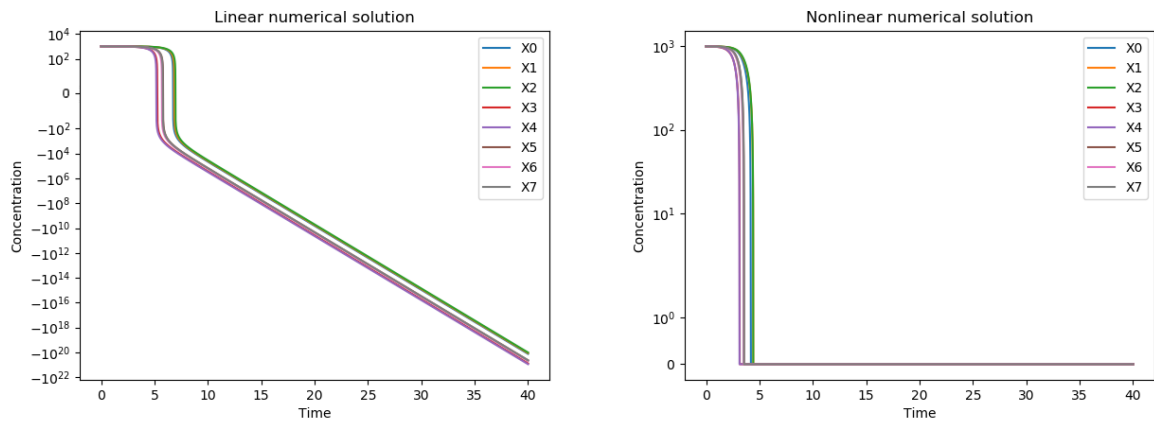
$A = \begin{bmatrix} A_1 & B \\ B^T & A_2 \end{bmatrix}$  where  $A_1$  and  $A_2$  are as follows:

$$A_1 = \begin{bmatrix} -W & 0.38 & 0.74 & 0.12 \\ 0.22 & -W & 0.34 & 0.16 \\ 0.44 & 0.21 & -W & 0.10 \\ 1.93 & 0.60 & 0.22 & -W \end{bmatrix}$$

$$A_2 = \begin{bmatrix} -W & 0.16 & 1.10 & 0.08 \\ 0.11 & -W & 0.89 & 0.36 \\ 0.54 & 0.24 & -W & 0.43 \\ 0.18 & 0.44 & 0.74 & -W \end{bmatrix}$$

In Figure 5.3a the linear solution is plotted, while in Figure 5.3b the nonlinear solution is plotted. The initial condition was chosen as  $\mathbf{x}_0 = 999$

In the linear case all concentrations diverge to  $-\infty$  already. The nonlinear model then simply stops the divergent behaviour at zero, and keeps the concentrations at zero.



(a) Linear numerical solution

(b) Nonlinear numerical solution

Figure 5.3: (a) Linear numerical solution for a strictly positive interaction matrix, apart from the diagonal which remains  $-W = -0.4$ . The initial condition  $\mathbf{x}_0 = 999$  is taken, instead of  $\mathbf{x}_0 = 1001$ . This results in a diverging solution to  $-\infty$ . (b) Nonlinear numerical solution for a strictly positive interaction matrix. All concentrations converge to 0. The solution shows stable behaviour.

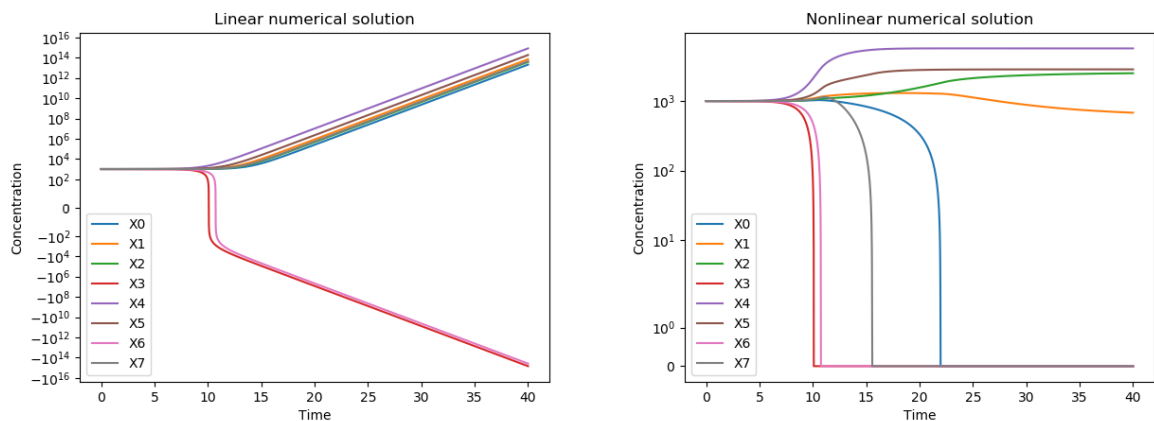
#### 5.1.4. Strictly Negative Interaction Matrix

The last of the list is the system with a strictly negative interaction matrix, Figure 4.21. The interaction matrix  $A$  is then given by

$$A = \begin{bmatrix} -|A_1| & -|B| \\ -|B^T| & -|A_2| \end{bmatrix}$$

In Figure 5.4a the linear solution is plotted and in Figure 5.4b the nonlinear solution. The linear case showed divergent behaviour in both directions. The concentrations diverging to  $+\infty$  cause a huge inhibitory effect, while the concentrations diverging to  $-\infty$  cause a huge excitatory effect. This was a flaw of the linear model.

In the nonlinear case some of the concentrations converge to a new equilibrium. Here the inhibitory effects on a certain concentration cancel out the excitatory effects. Again some concentrations become 0. The nonlinear model results in a stable solution, this is a big difference with the linear solution.



(a) Linear numerical solution

(b) Nonlinear numerical solution

Figure 5.4: (a) Linear numerical solution for a strictly negative interaction matrix. Some concentrations diverge to  $+\infty$ , others to  $-\infty$ . A large negative concentration with an inhibitory effect can cause a huge excitatory effect. (b) Nonlinear numerical solution for a strictly negative interaction matrix. Some concentrations converge to 0, other concentrations converge to another value. The solution shows stable behaviour.

The previous subsections have shown the numerical solutions of the nonlinear model for some cases. With these graphs in mind the working of the non-negative condition is hopefully clear. In the upcoming sections we will show some general properties of the nonlinear model.

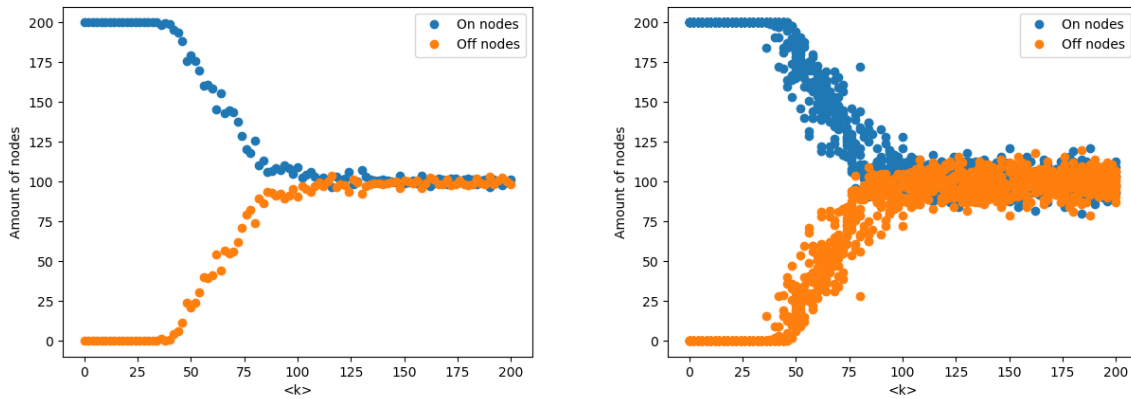
## 5.2. On and Off Distribution of Nodes

In this subsection we will treat the amount of on and off nodes in a network. These amounts play an important role in the estimation of the MLE.

Let us first define an on and off node. A node  $X_i$  is on if its concentration is positive, that is  $X_i > 0$ . A node  $X_i$  is off if its concentration is 0, that is  $X_i = 0$ . Numerically we will consider a node off, if the concentration  $X_i \leq 10^{-6}$  and on otherwise. The total number of on nodes is given by  $N_{on}$ , while the total amount of off nodes is denoted by  $N_{off}$ . The number of on and off nodes should add up to the total network size:  $N = N_{on} + N_{off}$ .

Is it possible to determine the amount of on nodes in a network depending on the average connectivity  $\langle k \rangle$ ? Where the average connectivity  $\langle k \rangle$  was defined as  $\langle k \rangle = \frac{L}{N}$ , with  $L$  the amount of non-zero entries and  $N$  the size of the network. It turns out that an estimation is possible for two cases of  $\langle k \rangle$ . If  $\langle k \rangle$  is small, then  $N_{on} \rightarrow N$ . If  $\langle k \rangle$  is 'large', then  $N_{on} \rightarrow \frac{1}{2}N$  (Stokić et al., 2008).

In Figure 5.5 the  $N_{on}$  and  $N_{off}$  are plotted against the average connectivity  $\langle k \rangle$ . These figures were created by generating 10 random matrices of size 200 with a certain connectivity  $\langle k \rangle$ . The random matrices have diagonal entries  $-0.6$  and the entries are taken from a  $N(0, 0.1^2)$  distribution. In Figure 5.14b we therefore obtain 10 values of  $N_{on}$  per  $\langle k \rangle$ . In Figure 5.14a we took the average of these 10 values per  $\langle k \rangle$ .



(a) Average  $N_{on}$  and  $N_{off}$  per  $\langle k \rangle$

(b)  $N_{on}$  and  $N_{off}$  per  $\langle k \rangle$

Figure 5.5: (a) The average amount of on nodes  $N_{on}$  vs the average connectivity  $\langle k \rangle$ . For small  $\langle k \rangle$ ,  $N_{on}$  goes to 200. For large  $\langle k \rangle$ ,  $N_{on}$  goes to 100 (b) The amount of nodes  $N_{on}$  vs the average connectivity  $\langle k \rangle$ . 10 data points per  $\langle k \rangle$  are collected and plotted.

The average plot shows the expected behaviour. For 'small'  $\langle k \rangle$ ,  $N_{on} = 200$ , while for 'large'  $\langle k \rangle$ ,  $N_{on} = \frac{1}{2}N = 100$ .

What is considered small and what is large? This is connected to the radius of Girko's circle. In equation 3.26 we found that the maximum Lyapunov exponent

$$MLE \approx \sigma(\sqrt{\langle k \rangle} - D) \quad (5.2)$$

where  $D = \frac{W}{\sigma}$ . So in our case  $D = \frac{0.6}{0.1} = 6$ .

This means that the largest expected real part of an eigenvalue (the MLE) is given by  $\sigma(\sqrt{\langle k \rangle} - 6)$ . If the  $MLE < 0$ , then all eigenvalues have negative real part and the system converges to its equilibrium,

such that all nodes remain on. As  $\sigma$  is positive, this happens if

$$\begin{aligned}\sqrt{\langle k \rangle} - 6 &< 0 \\ \sqrt{\langle k \rangle} &< 6 \\ \langle k \rangle &< 36\end{aligned}\tag{5.3}$$

Where we take the positive solution, since a negative average connectivity does not exist. In general we would obtain

$$\langle k \rangle < D^2.\tag{5.4}$$

So the average connectivity  $\langle k \rangle$  is small if  $\langle k \rangle < D^2$ .

Next we define a large average connectivity  $\langle k \rangle$ . For this we introduce the effective average connectivity:

$$\langle k_{on} \rangle = \langle k \rangle \frac{N_{on}}{N}\tag{5.5}$$

If we insert the effective average connectivity into the MLE equation 5.2 we receive

$$MLE \approx \sigma(\sqrt{\langle k_{on} \rangle} - D)\tag{5.6}$$

For large  $\langle k \rangle$  we had that  $N_{on} \rightarrow \frac{1}{2}N$ . Plugging this into the effective average connectivity, we get  $\langle k_{on} \rangle = \frac{\langle k \rangle}{2}$ . If we substitute this into equation 5.6 we obtain:

$$MLE \approx \sigma\left(\sqrt{\frac{\langle k \rangle}{2}} - D\right)\tag{5.7}$$

So, when does this approximation give  $MLE > 0$ ? That is if

$$\begin{aligned}\sqrt{\frac{\langle k \rangle}{2}} - D &> 0 \\ \sqrt{\frac{\langle k \rangle}{2}} &> D \\ \frac{\langle k \rangle}{2} &> D^2 \\ \langle k \rangle &> 2D^2\end{aligned}\tag{5.8}$$

Hence, a large average connectivity  $\langle k \rangle$  is when  $\langle k \rangle > 2D^2$ . Summarising, the small average connectivity is defined as  $\langle k \rangle < D^2$  and the large average connectivity as  $\langle k \rangle > 2D^2$ .

This leads to two critical values the small average connectivity gives  $MLE = 0$ , if  $\langle k \rangle = D^2$ , while the large average connectivity gives  $MLE = 0$ , if  $\langle k \rangle = 2D^2$ . These two critical values agree approximately with the small and large average connectivity and its corresponding  $N_{on}$  in figure 5.5. It is the region where  $N_{on}$  transfers from  $N_{on} = 200$  to  $N_{on} = 100$ . It is unknown how to calculate what the expected  $N_{on}$  is inside this region.

You might notice that it is by no means spot on. There can be several reasons for this. One, the network size is large but not infinite, so the eigenvalues do not perfectly converge to Girko's circle and its corresponding radius. Two, nodes can turn on and off as was seen in figure 5.1b. It is not known how quick  $N_{on}$  converges to a stable  $N_{on}$ , if it converges. So taking the  $N_{on}$  at a finite time  $t$  does not necessarily give the final  $N_{on}$  of the system. In Figure 5.6 this is shown.

In the next subsection we shall discuss the maximum Lyapunov exponent more thoroughly. The critical values  $\langle k \rangle = D^2$  and  $\langle k \rangle = 2D^2$  are then useful.

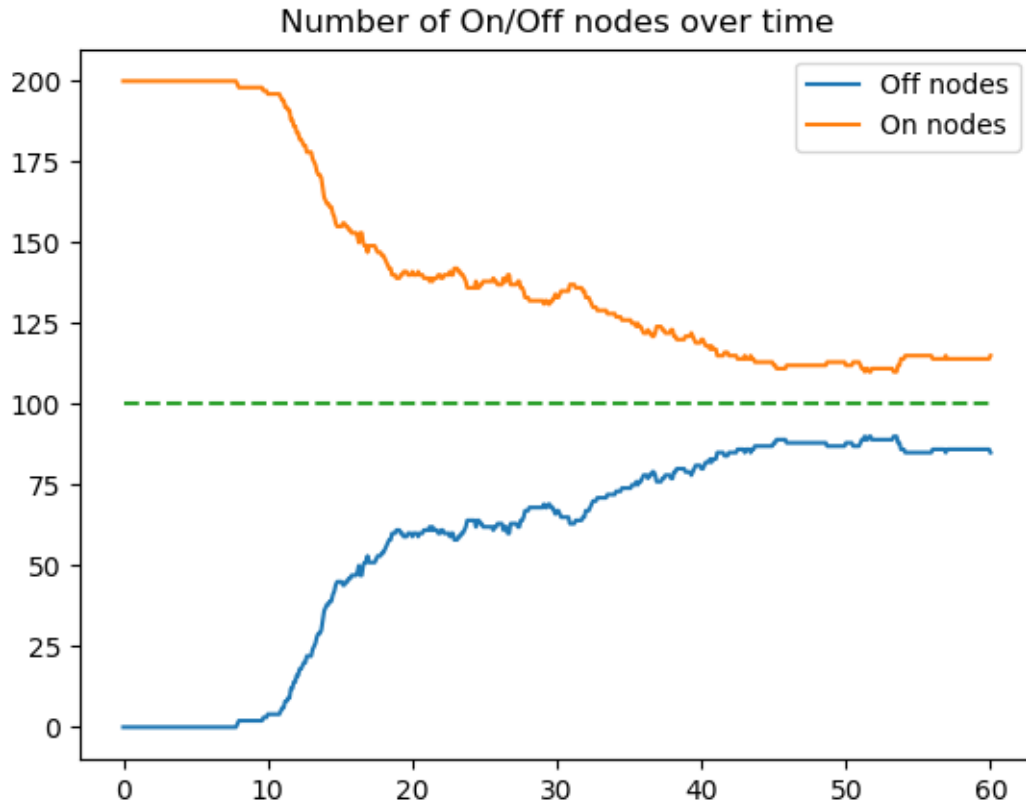


Figure 5.6: The number of on and off nodes over time for a matrix of size 200. These on/off numbers fluctuate over time. Taking the last  $N_{on}$  does not necessarily give the final  $N_{on}$  of the system.

### 5.3. Maximal Lyapunov Exponent

In this subsection the MLE is discussed. The MLE has been used many times throughout this report. Essentially, it is just a fancy word for the eigenvalue with the largest real part, as this eigenvalue determines the stability of the solution. In the linear model these eigenvalues could easily be calculated by using the interaction matrix.

However, in the nonlinear model the eigenvalues of the interaction matrix do not say much. For this the MLE is introduced, it turns out that it can be calculated in a numerical way. This MLE is then a simple measure for the stability of the solution of the nonlinear model.

The maximal Lyapunov exponent can be calculated numerically as follows (Stokić et al., 2008):

$$\lambda = \lim_{t \rightarrow \infty} \frac{1}{t} \ln \left( \frac{\|\mathbf{x}(t) - \mathbf{x}'(t)\|}{\|\mathbf{x}(0) - \mathbf{x}'(0)\|} \right) \quad (5.9)$$

where  $\mathbf{x}'(t)$  results from a small perturbation in the initial condition, such that  $\|\mathbf{x}(0) - \mathbf{x}'(0)\| < 1$ . In theory the time  $t$  should go to  $\infty$ , we have to settle for a finite time of course. In our numerical calculations we take 2000 steps with time step  $\Delta t = 0.1$ , the first 200 are discarded (Stokić et al., 2008).

#### 5.3.1. Edge of Chaos

In section 5.2 we calculated the two critical values  $\langle k \rangle = D^2$  and  $\langle k \rangle = 2D^2$ . At these critical values the MLE was expected to be 0. A MLE of zero, implies that our system is stable. It appears that in the region  $[D^2, 2D^2]$  a plateau of stable maximal Lyapunov exponents forms. This region depending on  $D$  is shown in figure 5.7.

If  $\langle k \rangle < D^2$ , a negative MLE is expected, in that case the system shows asymptotically stable behaviour. For  $\langle k \rangle > 2D^2$  a positive MLE is expected, then the system shows unstable behaviour. So, in this region a system can go from asymptotically behaviour, to stable behaviour, to unstable behaviour, if any changes in the effective average connectivity  $\langle k_{on} \rangle$  occur. The system lives on a so called 'edge of chaos'.

This is special, because in the linear case the stability of a system was deterministic. While in the nonlinear case it turns out that the stability can change over time. This might be an explanation for the fact that organisms evolve.

If all the mRNA concentrations are asymptotically stable, then no strands are turned off, and all the proteins remain available. No changes would occur in the organism. If the system is stable, some nodes turn off, but there are no crazy changes in concentrations. Then, there is enough room for evolution. At last the system could become unstable, then some strands of mRNA are highly present. Most of the times a sudden increase in some proteins or mRNA concentrations is caused by a defect. This is undesirable, think of a virus infection.

Concluding, to leave room for evolution, oscillatory behaviour is wishful.

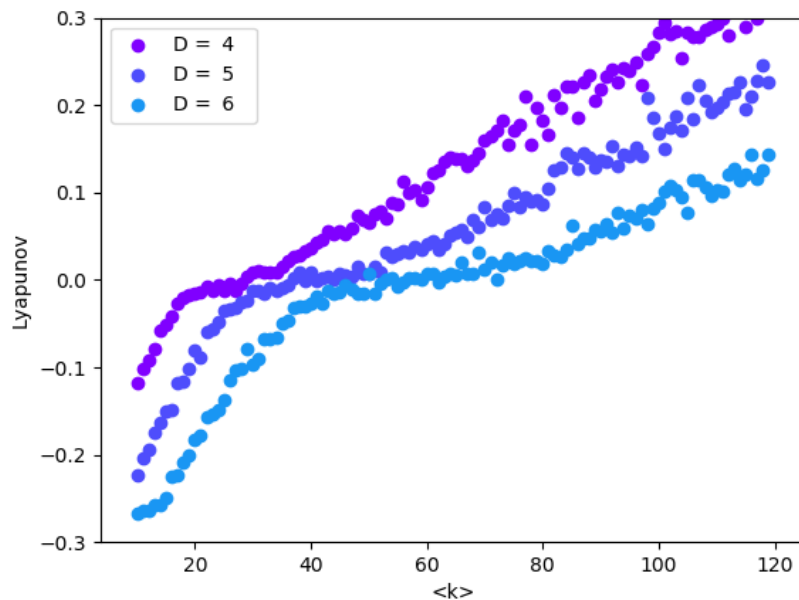


Figure 5.7: The plateau where the MLE is approximately 0 is formed from  $D^2$  to  $2D^2$ . The course of the MLE is plotted for different values of  $D$  vs the average  $\langle k \rangle$ . For  $D = 4$ , the region is  $16 \leq \langle k \rangle \leq 32$ . For  $D = 5$ , the region is  $25 \leq \langle k \rangle \leq 50$ . For  $D = 6$ , the region is  $36 \leq \langle k \rangle \leq 72$ .

### 5.3.2. Size of Network

How does the size of a network influence the edge of chaos? Above we have only shown the edge of chaos for a network that consists of 200 nodes. Does this plateau also form for smaller or larger networks?

The answer to this question is, yes, in general: the larger the network, the better the edge of chaos region. This is due to the fact that Girko's law holds for  $N \rightarrow \infty$ . So, if  $N$  is larger, then the eigenvalues converge better to the distribution of Girko's circle.

The numerical results from Figure 5.8 and Figure 5.9 support this statement. In these figures the course of the Lyapunov is plotted against the average connectivity  $\langle k \rangle$ . For both Figure (b) is a zoomed in graph of the plateau region. For Figure 5.8,  $D = 4$ , so the plateau forms around  $16 \leq \langle k \rangle \leq 32$ . While for Figure 5.9,  $D = 6$ , so the plateau forms around  $36 \leq \langle k \rangle \leq 72$ . For these figures 10 random matrices were generated with a certain average connectivity  $\langle k \rangle$ , after that the average Lyapunov of these 10 evaluations is taken. It should be noted that the Lyapunov is not exactly 0, but its maximum deviation in this region is  $|\lambda| < 0.05$ .

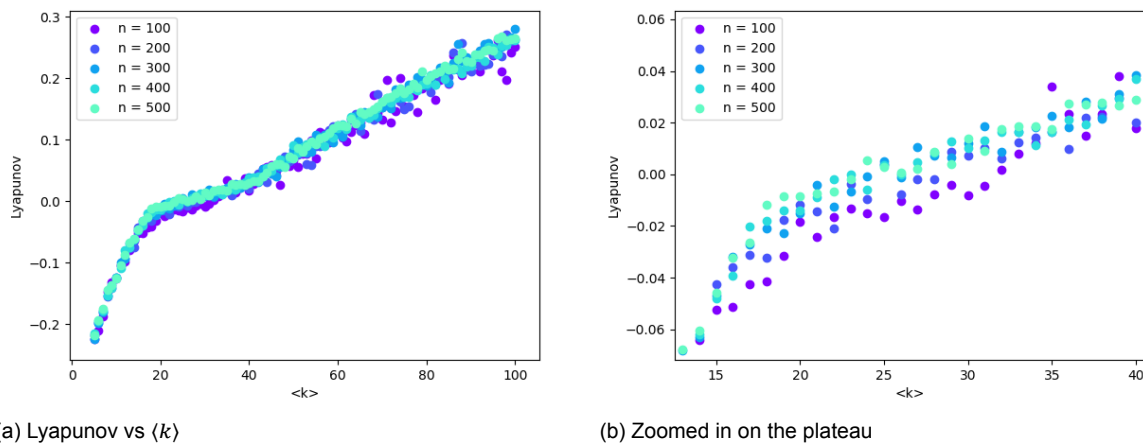


Figure 5.8: (a) Lyapunov vs average connectivity plot for  $D = 4$ . This is generated for different network sizes, see legend. (b) A zoom of the formed plateau around  $16 \leq \langle k \rangle \leq 32$ . The Lyapunov deviates at most  $|\lambda| < 0.05$ .

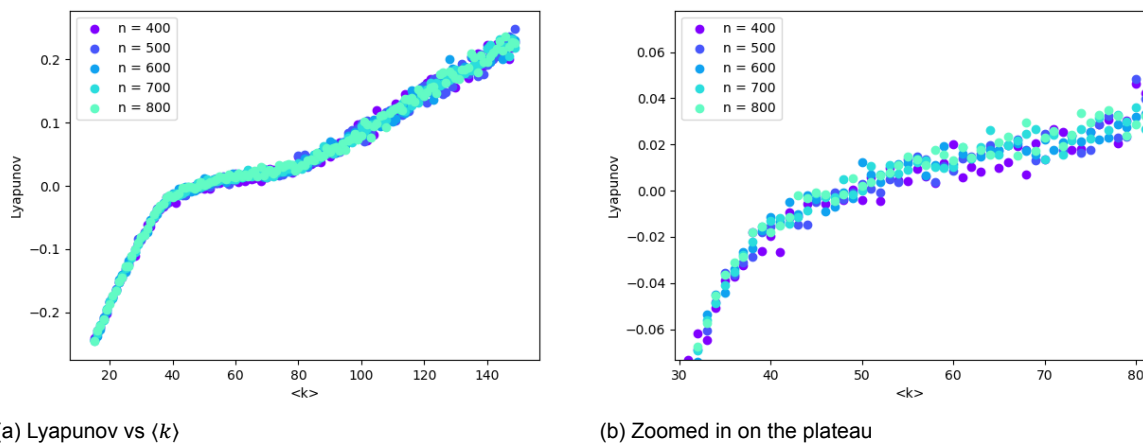


Figure 5.9: (a) Lyapunov vs average connectivity plot for  $D = 6$ . This is generated for different network sizes, see legend. (b) A zoom of the formed plateau around  $36 \leq \langle k \rangle \leq 72$ . The Lyapunov deviates at most  $|\lambda| < 0.04$ .

### 5.3.3. Weight and Amount of Interconnections

How do interconnections influence the edge of chaos? To answer this question we will look at the influence of the weight of an interconnection and the amount of interconnections.

Let us first consider the weight of an interconnection. In the linear model an interconnection of weight  $\epsilon$  caused an eigenvalue of approximately  $\epsilon$ . This does not seem to hold for the MLE of the nonlinear model anymore. For one interconnection with a small weight the plateau still forms perfectly. See Figure 5.10a.

If, we however increase the magnitude of the weight, the plateau around 0 will disappear. This seems to happen from an interconnection with weight  $\epsilon = 0.7$  and onwards. Which is visible in Figure 5.10b.

These figures were created by generating 10 random matrices with average connectivity  $\langle k \rangle$  and of size  $400 \times 400$ , which consists of 2 networks each of 200 nodes. After that, the average is taken. The interaction rates were taken from a  $N(0, 0.1^2)$  distribution. The interconnections of weight  $\epsilon$  were added on a random location.

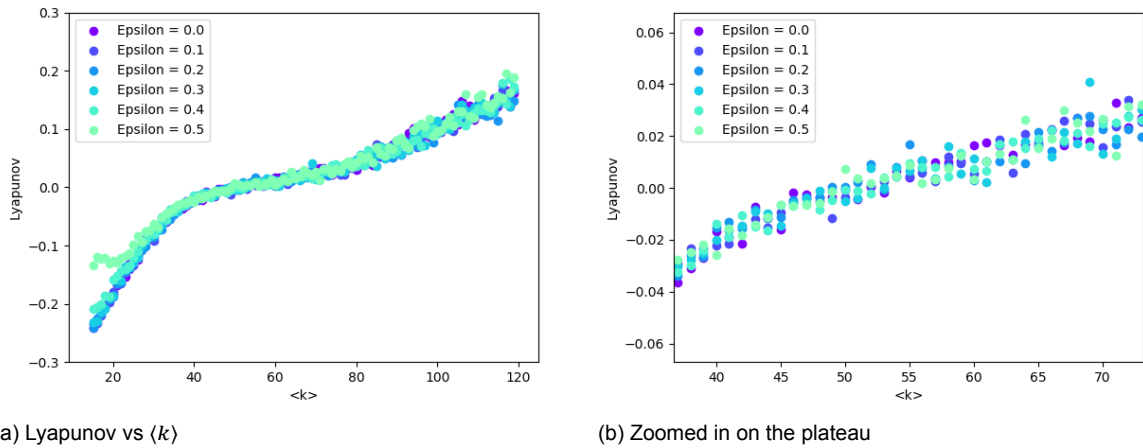


Figure 5.10: (a) Lyapunov vs average connectivity plotted for several weights  $\epsilon$  for one interconnection. This interconnection is randomly placed. The system consists of 2 networks of 200 nodes and  $D = 6$  (b) A zoom of the formed platform  $36 \leq \langle k \rangle \leq 72$ . The Lyapunov deviates at most  $|\lambda| < 0.04$ .

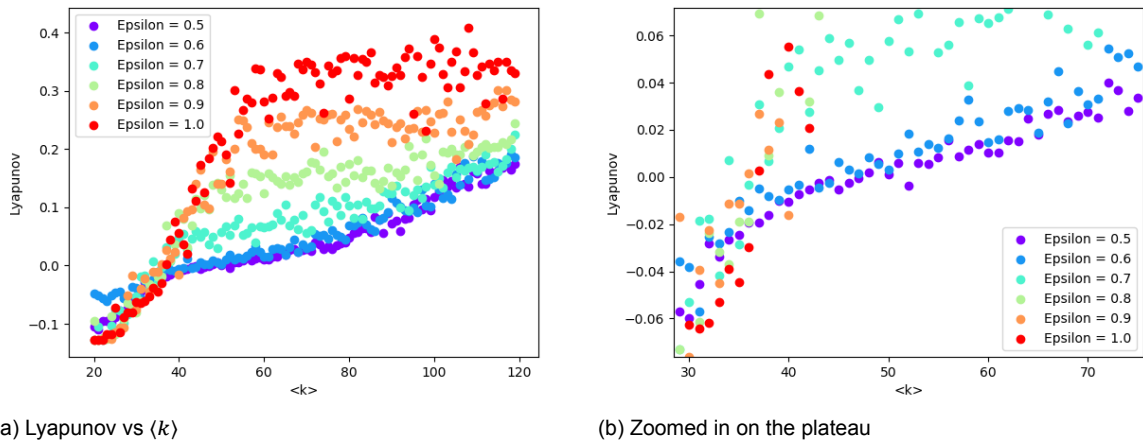
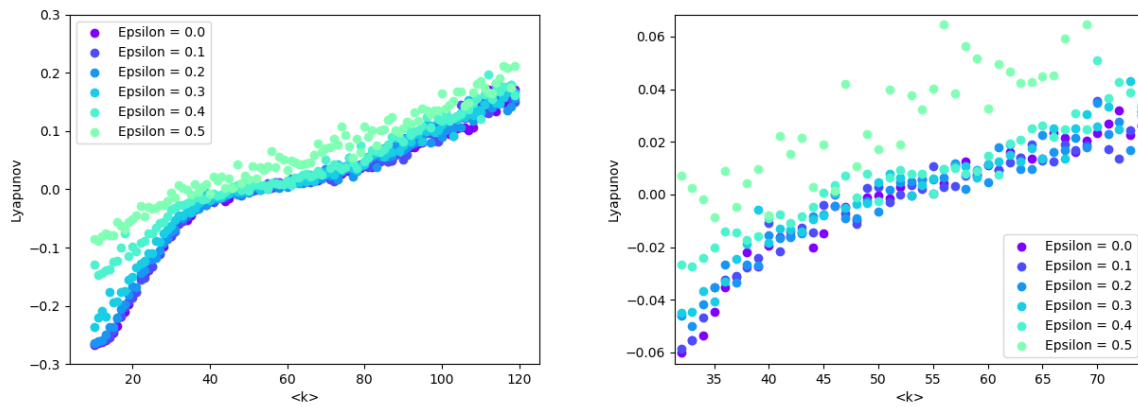


Figure 5.11: (a) Lyapunov vs average connectivity plotted for several weights  $\epsilon$  for one interconnection. This interconnection is randomly placed. The system consists of 2 networks of 200 nodes and  $D = 6$  (b) A zoom of the region where the platform is expected  $36 \leq \langle k \rangle \leq 72$ . The Lyapunov deviates at most  $|\lambda| < 0.04$  for  $\epsilon = 0.5$  or  $\epsilon = 0.6$ . For large weights the platform disappears.

Now, let us take a look at the influence of the amount of interconnections. In this case 10 interconnections of weight  $\epsilon$  are added randomly. The figures are similarly generated as before. In the linear case the exact influence of the amount of interconnections and the placement of these interconnections was unknown. It is known that outliers existed.

In Figure 5.12 it is visible that the plateau disappears for  $\epsilon = 0.5$ . With the knowledge of the influence of the weight on the MLE, it is expected that for bigger weights of  $\epsilon$  this plateau will also disappear. The influence of the amount of interconnections is also here hard to check, as the placement of the interconnections also affected the eigenvalue distribution of the linear model. It is however clear from this figure that also the amount of interconnections does influence the Lyapunov exponent, as the Lyapunov changes for small values of  $\langle k \rangle$  compared to Figure 5.10a.



(a) Lyapunov vs  $\langle k \rangle$

(b) Zoomed in on the plateau

Figure 5.12: (a) Lyapunov vs average connectivity plotted for several weights  $\epsilon$  with 10 bidirectional interconnections. These are randomly placed. The system consists of 2 networks of 200 nodes and  $D = 6$ . The platform shows till  $\epsilon = 0.4$ . For  $\epsilon = 0.5$  the platform disappears. (b) A zoom of the formed platform  $36 \leq \langle k \rangle \leq 72$ . The Lyapunov deviates at most  $|\lambda| < 0.06$ .

### 5.4. Initial Condition

At last, we might ask whether the initial condition for the mRNA concentrations has an influence on the plateau. Unexpectedly, it was discovered that the plateau does change for certain initial conditions. In Figure 5.13 it is visible that the plateau is shifted for the initial conditions close to the equilibrium,  $\mathbf{x}_0 = 999$  and  $\mathbf{x}_0 = 1001$ . It is strange that the plateau seems to form around  $\lambda = 0.5$  instead of  $\lambda = 0$ .

A possible explanation for this is that the equilibrium  $\mathbf{x}^0$  is an unstable saddle point. Solutions that are close to this equilibrium want to leave the unstable saddle point as quick as possible. The solution with initial condition  $\mathbf{x}_0 + 0.01$  can then differ a lot from the solution with initial condition  $\mathbf{x}_0$ . This perturbed solution is required to calculate the maximal Lyapunov exponent.

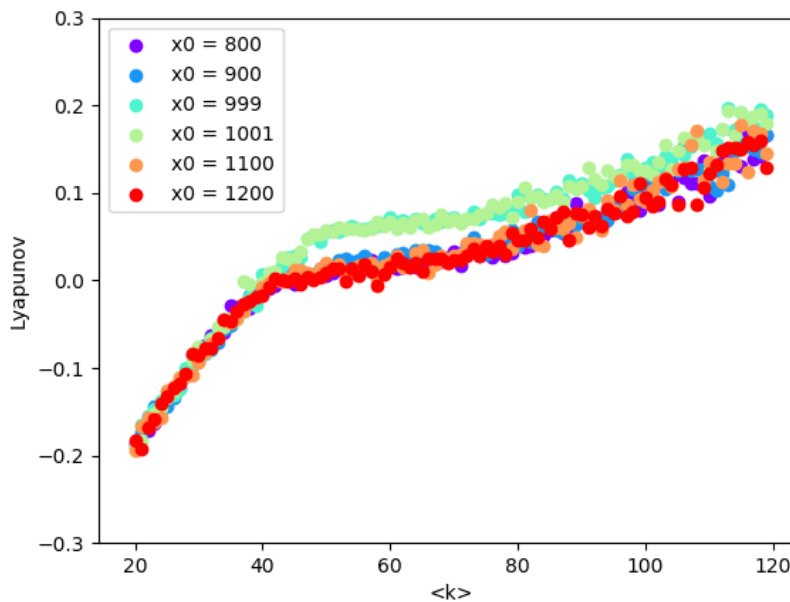
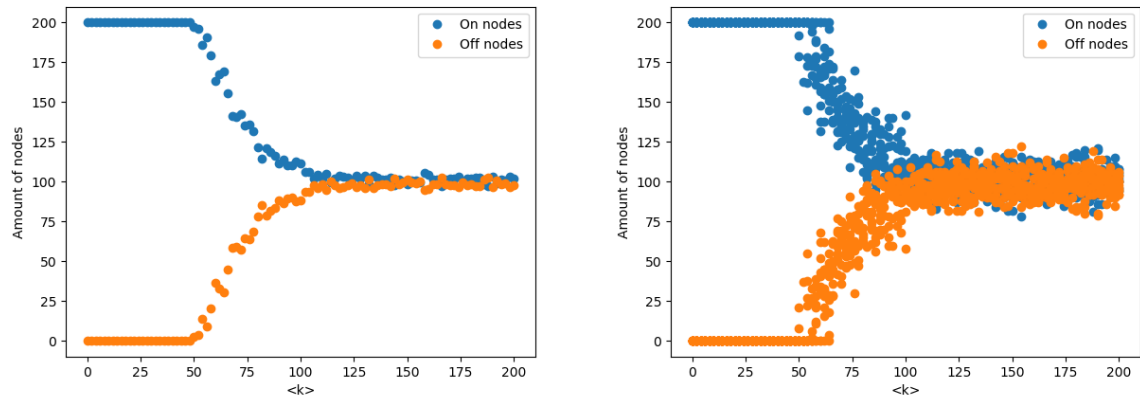


Figure 5.13: Lyapunov vs average connectivity  $\langle k \rangle$  plotted for different initial conditions  $\mathbf{x}_0$ . There forms a platform around 0 for  $36 \leq \langle k \rangle \leq 72$  for initial conditions that deviate far from the equilibrium  $\mathbf{x}^0 = 1000$ . For initial conditions around the equilibrium,  $\mathbf{x}_0 = 999$  and  $\mathbf{x}_0 = 1001$  a different platform around  $\lambda = 0.05$  forms for  $50 \leq \langle k \rangle \leq 80$

This does not seem to be due to a numerical error since the development of the  $N_{on}$  graph (Figure 5.14) is also different, if it is compared to Figure 5.5. The course of  $N_{on}$  also shifts a bit to the right, as the transition starts around  $\langle k \rangle = 50$ , instead of  $\langle k \rangle = 36$ .



(a) Average  $N_{on}$  and  $N_{off}$  per  $\langle k \rangle$

(b)  $N_{on}$  and  $N_{off}$  per  $\langle k \rangle$

Figure 5.14: (a) The average amount of on nodes  $N_{on}$  vs the average connectivity  $\langle k \rangle$  with  $D = 6$ , and  $\mathbf{x}_0 = 999$ . For small  $\langle k \rangle$ , up to  $\langle k \rangle = 50$ ,  $N_{on}$  goes to 200. This is different from the critical value  $\langle k \rangle = 36$ . For large  $\langle k \rangle$ ,  $N_{on}$  goes to 100 (b) The amount of nodes  $N_{on}$  vs the average connectivity  $\langle k \rangle$ . 10 data points per  $\langle k \rangle$  are collected and plotted. Big deviations are possible, since it is not known how quick the  $N_{on}$  converges to a stable  $N_{on}$  value.

# 6

## Discussion

In this section some results from the linear and nonlinear model are discussed, if it has not been discussed in the section itself yet. Let us start with the linear model.

During the linear model only the same  $8 \times 8$  network was shown. All figures were about this matrix. In general we have checked that the same results hold for larger networks. This particular example was chosen, such that the numerical solution can be plotted, such that the interaction matrix can be written down and such that it is possible to check that the numerical solution agrees with the analytical solution by reasoning with the eigenvalues and eigenvectors. If a larger network is chosen, then the graphs become too messy. It should be noted that Girko's law does not always hold for small matrices. This was visible in the histograms Figure 4.14 and Figure 4.15. The real components of B do not converge to Wigner's semicircle. This would have worked for a larger system.

From now on the nonlinear model will be discussed. In section 5.3 the MLE was introduced. The numerical solution here actually requires our time  $t \rightarrow \infty$ . We took 2000 steps with time step  $\Delta t = 0.1$  and perturbation 0.01. With this the plateau around 0 shows. However the plateau from the article (Stokić et al., 2008) obtained a precision of  $|\lambda| < 0.005$ . This is a big difference compared to our results, we got a precision of  $|\lambda| < 0.05$ . What could cause these difference? There are several differences between this report and the article. In the article they took 1000 steps, we take 2000 steps. In the article they took  $\sigma = 1$  and  $D = 4$  as diagonal elements, we use  $\sigma = 0.1$  and  $W = 0.4$  as diagonal elements. Their initial perturbation could not be found. Besides these differences the article took the average over 50 random realisations of networks for a given parameter set. We took the average over 10 random realisations of networks, due to calculation times. It is likely that all these differences explain the difference with our case.





# Conclusion

The purpose of this report was to study the stability of the model for the gene pools of interacting organisms. To do so two models were evaluated. The linear model, and the linear model with a 'non-negative concentration'-constraint, which is the nonlinear model. The eigenvalue distribution was, in some cases, found by using Girko's law from random matrix theory. This law states that the normalised eigenvalues are distributed on a unit circle in the complex plane.

## 7.1. Linear Model

First, we will answer the linear model. Given a random interaction matrix A of the form

$$\begin{bmatrix} A_1 & B \\ B^T & A_2 \end{bmatrix}$$

where the matrices  $A_1$  and  $A_2$  can be envisioned to model a certain gene pool that corresponds to an organism, and  $B$  and  $B^T$  represent the interactions between the two organisms, here  $B^T$  denotes the transpose of  $B$ .

It was found that the stability of the linear model is deterministic. In the sense that once the eigenvalues of the interaction matrix A are found, the stability is determined.

However, the form of matrix B has a huge influence on the distribution of the eigenvalues, this depends on the strength of the interactions between the two organisms. A large strength causes the system to become inevitably unstable, while a small strength does not influence the stability of the system at all.

A one-sided interaction - where organism 1 only interacts with organism 2 and there is no interaction from organism 2 to organism 1 - does not influence the stability of the system.

As last, the number of interactions between organism 1 and organism 2, and the placement of these interactions have an influence on the stability of the system. But, this is mostly connected to the strength of the interaction as well. So, depending on the strength this could make the system unstable, which is related to a large strength, while a small strength does again nothing to the stability of the system.

## 7.2. Nonlinear Model

Second, the nonlinear model. This is essentially the linear model, but then with the added constraint: concentrations are non-negative. It was found that the stability of a system is not necessarily deterministic. The system can be partly asymptotically stable, partly stable and partly unstable for different time windows. It is living on the 'edge of chaos'. The edge of chaos is a plateau where the solution is stable. Due to this, a statement as "a large strength causes the system to be unstable" can not be given.

The remaining results are more complex. To understand this some notation is required, which is

treated in chapter 2. There are some interesting results about the plateau edge of chaos. The length of this stability plateau is given by  $[D^2, 2D^2]$ , where  $D = \frac{W}{\sigma}$ , with  $W$  the diagonal elements of  $A$ . The plateau becomes more stable for larger interaction matrices  $A$ . The plateau is influenced by the form of matrix  $B$ . A large strength causes the plateau to disappear. At last, the plateau is influenced by the initial concentrations of the mRNA. An initial condition close to the equilibrium, causes the plateau to disappear around 0. In general the stability of the system depends on the average connectivity  $\langle k \rangle$ , which can change over time due to nodes turning on or off.

### 7.3. Recommendations

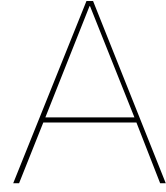
To anyone who is interested in researching this topic, we wish to add the following four suggestions for future research:

As you might have noticed most of the results given in this report are numerical instead of theoretical. Future research on this subject could use some more qualitative results. It is for example currently unknown how the eigenvalues are exactly affected by the interconnection matrix  $B$ , while this plays a very important role in the stability of a system. The hand-waving proof in this report used the characteristic polynomial. For smaller matrices it is possible to reason with this, but for larger matrices this is impossible. Another technique should be used, which is unknown due to the added complexity of the placement of an interconnection.

In this report we considered several cases of adding an interconnection. There are more possibilities: adding interconnections with an inhibitory effect, adding multiple interconnections of different weights or adding directed interconnections on different places from network 1 to 2 and 2 to 1. What might also be interesting is connecting more than 2 networks, where for example network 1 is connected to network 3, and network 3 is connected to network 2.

The original model (Stokić et al., 2008) was a SDE. In this report this SDE was reduced to a simple linear ODE. It might be interesting to see how the SDE model behaves under the adding of interconnections. Although we expect that the results remain the same.

Another way of looking at a network is from a topological point of view. It could be interesting to give concepts like “clustering”, “Error Tolerance”, “Attack Tolerance”, “Percolation Threshold” and “Fragmentation” in combination with interacting organisms a thought. Maybe this gives some new insights.



# Notes on the Proof of Wigner's Semicircle

In this part we will show why equation 3.7 holds. Mind that the notation of indices is a bit different.

$$\frac{1}{N} \sum_{i=1}^N \frac{1}{z - \lambda_i} = \sum_{k=0}^{\infty} \frac{1}{z^{k+1}} \frac{1}{N} \text{Tr}(A^k) \quad (\text{A.1})$$

We begin by writing down the geometric series of  $\frac{1}{z - \lambda_i}$ , for  $z$  sufficiently large.

$$\begin{aligned} \frac{1}{z - \lambda_k} &= \frac{1}{z} \cdot \frac{1}{1 - \frac{\lambda_i}{z}} \quad \left| \frac{\lambda_i}{z} \right| < 1 \\ &= \frac{1}{z} \sum_{n=0}^{\infty} \left( \frac{\lambda_i}{z} \right)^n \\ &= \sum_{n=0}^{\infty} \frac{1}{z^{n+1}} \cdot (\lambda_i)^n \end{aligned} \quad (\text{A.2})$$

Plugging this into the LHS of equation A.1 gives:

$$\begin{aligned} \frac{1}{N} \sum_{i=1}^N \frac{1}{z - \lambda_i} &= \frac{1}{N} \sum_{i=1}^N \sum_{n=0}^{\infty} \frac{1}{z^{n+1}} \cdot (\lambda_i)^n \\ &= \frac{1}{N} \sum_{n=0}^{\infty} \frac{1}{z^{n+1}} \sum_{i=1}^N (\lambda_i)^n \\ &= \frac{1}{N} \sum_{n=0}^{\infty} \frac{1}{z^{n+1}} \text{Tr}(A^n) \end{aligned} \quad (\text{A.3})$$

Replacing the indices  $n$  with a  $k$  gives the RHS of equation A.1. The last equal sign ( $=$ ) holds, because of the cyclic property of traces and the fact that the sum of eigenvalues equals the trace of a matrix, independent of its basis. So, if  $A = PDP^{-1}$ , with  $D$  an upper triangular matrix, then  $A^n = PD^nP^{-1}$

$$\begin{aligned} \text{Tr}(A^n) &= \text{Tr}(PD^nP^{-1}) \\ &= \text{Tr}(P^{-1}PD^n) \quad \text{Cyclic property} \\ &= \text{Tr}(D^n) \\ &= \sum_{i=1}^N (\lambda_i)^n \end{aligned} \quad (\text{A.4})$$

In this part we will show why

$$\mathbb{E} \left( M_{11} - \sum_{k,l=1}^{N-1} [M_{12}]_{1k} [m^{-1}]_{kl} [M_{21}]_{l1} \right) = \mathbb{E}(M_{11}) - \frac{\sigma^2}{N} \cdot \mathbb{E} \text{Tr}(m^{-1}) \quad (\text{A.5})$$

To show this the following properties of expectation are required

1. Linearity:  $\mathbb{E}(X + Y) = \mathbb{E}(X) + \mathbb{E}(Y)$
2. Product of independent random variables:  $\mathbb{E}(XY) = \mathbb{E}(X)\mathbb{E}(Y)$

By the definition of a Wigner matrix we had that all off diagonal entries are iid Gaussian random variables with mean 0 and variance  $\frac{\sigma^2}{N}$ . The diagonal entries are iid Gaussian random variables with mean 0 and variance  $\frac{2\sigma^2}{N}$ . A Wigner matrix is also symmetric, so  $x_{ij} = x_{ji}$ . This is used to reason the following for the entries  $[M_{12}]_{1k}$  and  $[M_{21}]_{l1}$

1.  $[M_{12}]_{1k} = [M_{21}]_{l1} = (\text{say}) W$  if  $k = l$
2.  $[M_{12}]_{1k}$  and  $[M_{21}]_{l1}$  are independent if  $k \neq l$

By the symmetry (1.), this implies that  $\mathbb{E}([M_{12}]_{1k}[M_{21}]_{l1}) = \mathbb{E}(W^2)$ , if  $k = l$

Using the definition of variance and  $\mathbb{E}(W) = 0$ :  $\text{var}(W) = \mathbb{E}(W^2) - \mathbb{E}(W)^2 \Rightarrow \mathbb{E}(W^2) = \text{var}(W) = \frac{\sigma^2}{N}$

By independence (2.), this implies that  $\mathbb{E}([M_{12}]_{1k}[M_{21}]_{l1}) = \mathbb{E}([M_{12}]_{1k})\mathbb{E}([M_{21}]_{l1}) = 0$ , if  $k \neq l$

Also note that the vectors  $[M_{12}]_{1k}$  and  $[M_{21}]_{l1}$  are always independent of  $[m^{-1}]_{kl}$ . These properties can now be used to reduce  $\mathbb{E}(M_{11} - \sum_{k,l=1}^{N-1} [M_{12}]_{1k} [m^{-1}]_{kl} [M_{21}]_{l1}) =$

$$\begin{aligned} & \mathbb{E}(M_{11}) - \sum_{k,l=1}^{N-1} \mathbb{E}([M_{12}]_{1k} [m^{-1}]_{kl} [M_{21}]_{l1}) = \\ & \mathbb{E}(M_{11}) - \sum_{k=l=1}^{N-1} \mathbb{E}([M_{12}]_{1k} [m^{-1}]_{kl} [M_{21}]_{l1}) - \sum_{k \neq l=1}^{N-1} \mathbb{E}([M_{12}]_{1k} [m^{-1}]_{kl} [M_{21}]_{l1}) = \\ & \mathbb{E}(M_{11}) - \sum_{k=l=1}^{N-1} \mathbb{E}([M_{12}]_{1k} [M_{21}]_{k1}) \mathbb{E}([m^{-1}]_{kk}) - \sum_{k \neq l=1}^{N-1} \mathbb{E}([M_{12}]_{1k}) \mathbb{E}([m^{-1}]_{kl}) \mathbb{E}([M_{21}]_{l1}) = \\ & \mathbb{E}(M_{11}) - \frac{\sigma^2}{N} \sum_{k=l=1}^{N-1} \mathbb{E}([m^{-1}]_{kk}) - 0 = \\ & \mathbb{E}(M_{11}) - \frac{\sigma^2}{N} \mathbb{E} \left( \sum_{k=l=1}^{N-1} [m^{-1}]_{kk} \right) = \\ & \mathbb{E}(M_{11}) - \frac{\sigma^2}{N} \mathbb{E}(\text{Tr}(m^{-1})) \end{aligned} \quad (\text{A.6})$$

In this part we will show that  $g = \frac{z - \sqrt{z^2 - 4\sigma^2}}{2\sigma^2} \sim \frac{1}{z}$ . For this we will need the Maclaurin series of  $\sqrt{1-x}$ , or simply the Taylor series around 0.

$$\sqrt{1-x} \approx 1 - \frac{1}{2}x \quad (\text{A.7})$$

By factoring a  $z$  and plugging in the Taylor series we obtain

$$\begin{aligned} g &= \frac{z - \sqrt{z^2 - 4\sigma^2}}{2\sigma^2} \\ &= \frac{z - z\sqrt{1 - \frac{4\sigma^2}{z^2}}}{2\sigma^2} \\ &\approx \frac{z - z(1 - \frac{1}{2}\frac{4\sigma^2}{z^2})}{2\sigma^2} \end{aligned} \quad (\text{A.8})$$

Where the latter can be reduced to

$$\frac{z - z(1 - \frac{1}{2}\frac{4\sigma^2}{z^2})}{2\sigma^2} = \frac{z - z + \frac{2\sigma^2}{z}}{2\sigma^2} = \frac{1}{z} \quad (\text{A.9})$$

Hence our result  $g = \frac{z - \sqrt{z^2 - 4\sigma^2}}{2\sigma^2} \sim \frac{1}{z}$ .



# Bibliography

- Bose, A., Chatterjee, S., & Gangopadhyay, S. (2003). Limiting spectral distributions of large dimensional random matrices, 2. <https://statweb.stanford.edu/~souravc/jisarev.pdf>
- Feier, A. (2012). Methods of proof in random matrix theory [Bachelor's Thesis]. <https://www.math.harvard.edu/media/feier.pdf>
- Jeong, H., Mason, S., Barabási, A., & Oltvai, Z. (2001). Lethality and centrality in protein networks. *Nature*, 411, 41–42. <https://doi.org/10.1038/35075138>
- Potters, M., & Bouchaud, J. (2020). *A first course in random matrix theory*. Cambridge University Press.
- Sadun, L. (2008). *Applied linear algebra* (2nd ed.). American Mathematical Society.
- Sanders, J. (2020). The influence of network topology on the dynamics of gene regulatory networks [Bachelor's Thesis]. <https://repository.tudelft.nl/>
- Stokić, D., Hanel, R., & Thurner, S. (2008). Inflation of the edge of chaos in a simple model of gene interaction networks. *Physical Review E*, 77(6). <https://doi.org/10.1103/physreve.77.061917>
- Tao, T. (2010). 254a, notes 4: The semi-circular law. <https://terrytao.wordpress.com/2010/02/02/254a-notes-4-the-semi-circular-law/>
- Tao, T. (2013). Outliers in the spectrum of iid matrices with bounded rank perturbations. *Probability Theory and Related Fields*, 155, 231–263. <https://doi.org/10.1007/s00440-011-0397-9>